*J. Physiol.* (1987), **387**, *pp.* 519–548
*With* 16 *text-figures*
*Printed in Great Britain*



# POTASSIUM CURRENTS EVOKED BY BRIEF DEPOLARIZATIONS IN BULL-FROG SYMPATHETIC GANGLION CELLS

BY B. LANCASTER* AND P. PENNEFATHER†

*From the Department of Neurobiology and Behaviour, State University of New York, Stony Brook, NY 11794, U.S.A.*

(*Received 13 March 1986*)

SUMMARY

1. Sympathetic neurones of the bull-frog *Rana catesbeiana* were subjected to a two-electrode voltage-clamp technique in order to investigate the $K^+$ currents which can be elicited by action potentials or similar brief depolarizations.

2. Four separate $K^+$ currents were observed ($I_C$, $I_K$, $I_{AHP}$ and $I_M$). These could be separated on the basis of voltage sensitivity, $Ca^{2+}$ dependence and deactivation kinetics.

3. Two of these currents, which were clearly activated by an action potential, were $Ca^{2+}$ dependent. A voltage- and TEA (tetraethylammonium)-sensitive $K^+$ current, $I_C$, was activated within the first 1–2 ms of a depolarizing command. This current decayed on average with a time constant of 2·4 ms at −40 mV. The maximal conductance was outside the range which could be adequately voltage clamped but, as much as 2 $\mu$S could be activated by brief (2–3 ms) commands. Activation of $I_C$ during an action potential accounts for the $Ca^{2+}$ dependence of the repolarization. $I_C$ did not exhibit a transient component.

4. A second $Ca^{2+}$-dependent $K^+$ current, $I_{AHP}$, was also activated after as little as 1 ms depolarization but was not voltage sensitive and was much less sensitive to TEA. The current decayed with a time constant of around 150 ms at −40 mV. The maximal conductance was about 30 nS.

5. The voltage-sensitive delayed rectifying current, $I_K$, made a contribution to the total $K^+$ conductance of the cell similar to $I_C$ in magnitude; however, the current is not activated within the normal voltage range or time course of an action potential. The current decayed on average with a time constant of 21 ms at −40 mV.

6. $I_M$, a muscarine- and voltage-sensitive current, is not activated to any significant degree by a single action potential. The data further imply that the rate of opening of the ion channels mediating $I_M$ is less voltage sensitive than the rate of closing.

7. Large changes in the $K^+$ reversal potential occur following depolarizing commands which evoke large $K^+$ currents. This is attributed to $K^+$ accumulation within a restricted extracellular space. Extracellular $K^+$ may double or even triple during a single action potential.

* Present address: Department of Pharmacology, University of California Medical School, San Francisco, CA 94143, U.S.A.

† Present address: Faculty of Pharmacy, University of Toronto, 19 Russell Street, Toronto, Ontario M5S 1A1, Canada.

## INTRODUCTION

Bull-frog sympathetic ganglion B neurones contain at least four different $K^+$ currents ($I_C$, $I_K$, $I_{AHP}$ and $I_M$) that play roles in determining action potential shape and threshold (Adams, Jones, Pennefather, Brown, Koch & Lancaster, 1986). Inhibition of $Ca^{2+}$ influx prolongs the repolarizing phase of action potentials in these cells (Adams, Constanti, Brown & Clark, 1982*c*; MacDermott & Weight, 1982). This implies that the classical delayed $K^+$ current which causes spike repolarization in axons (Hodgkin & Huxley, 1952; Frankenhaeuser, 1962) is not solely responsible for this event in the somata of bull-frog ganglion cells. Indeed a large $Ca^{2+}$-dependent $K^+$ current ($I_C$) has been observed in this cell (Adams *et al.* 1982*c*). The current is produced by a voltage- and $Ca^{2+}$-dependent channel that has pharmacological and single-channel properties very similar to a large-conductance $K^+$ channel that has been observed in a variety of cell types (see Marty, 1981; Pallotta, Magleby & Barrett, 1981; Adams *et al.* 1982*c*). $Ca^{2+}$-dependent outward currents can be generated by single action potentials in other systems (Gorman & Thomas, 1980; Storm, 1985). However, B neurones of the bull-frog ganglion (see Dodd & Horn, 1983) are particularly well suited to study the relative importance of such currents in spike repolarization. First, a reasonable number of the cells endure twin impalements which permit voltage clamping with the necessary temporal resolution and voltage control to study the rapidly activating $K^+$ currents which may underlie spike repolarization. Secondly, they lack dendrites (Taxi, 1976; Wantanabe, 1983) so that spatial inhomogeneities in membrane potential will be less pronounced than in other preparations.

A principle aim, therefore, was to estimate the relative contributions of $I_C$ and delayed rectifier (henceforth called $I_K$) in action potential repolarization. This was carried out by giving large, but brief, depolarizing commands which effectively mimicked the voltage trajectory of an action potential. The outward currents generated by these voltage jumps were separated according to $Ca^{2+}$ dependence, voltage sensitivity and kinetics. Since the $Na^+$ current ($I_{Na}$) inactivates rapidly (Jones, 1985) and the $Ca^{2+}$ current ($I_{Ca}$) is no more than a few nanoamperes (Adams, Brown & Constanti, 1982*b*). The magnitude of the large outward currents are fairly direct measures of $K^+$ currents activated by brief voltage-clamp commands.

The protocol was chosen to cover the voltage range over which action potentials can be observed, i.e. $-40$ mV to further depolarized potentials. Particular attention was paid to currents evoked between 0 and $+40$ mV since this is clearly the range in which spike repolarization is initiated and also where very large outward currents are activated with little delay. There are several types of outward currents other than $I_C$ and $I_K$ that can be activated in B cells by depolarization. They are much smaller and unlikely to play a major role in repolarization of the action potential. $I_M$ is a voltage-dependent $K^+$ current that is coupled to muscarinic receptors (Adams, Brown & Constanti, 1982*a*). $I_{AHP}$ is a voltage-independent $K^+$ current that is activated by intracellular $Ca^{2+}$. In contrast to $I_C$ it is resistant to TEA (tetraethylammonium) and blocked by apamin (Pennefather, Lancaster, Adams & Nicoll, 1985*b*). Although relatively small, these two currents deactivate much more slowly than $I_C$ or $I_K$ so that, if activated by one action potential, they can influence the threshold of subsequent action potentials. In view of the importance of these two currents in regulating

repetitive firing (see Pennefather, Jones & Adams, 1985*a*; Adams *et al.* 1986), our experiments also addressed the question of the degree to which short voltage jumps can activate $I_M$ and $I_{AHP}$. Other small $K^+$ currents known to be present in B cells (e.g. A current and transient $Ca^{2+}$-dependent outward currents) are mostly inactivated at $-40$ mV (Adams *et al.* 1982*a*; MacDermott & Weight, 1982) and thus do not further complicate our analysis.

During the course of this work, we obtained indirect evidence for a number of interesting phenomena that complicate the interpretation of our results. For example, the kinetics of $I_K$ appeared to be sensitive to removal of extracellular $Ca^{2+}$ (see also Armstrong & Matteson, 1986) or addition of extracellular $K^+$ (see also Dubois, 1981). With brief commands, $Ca^{2+}$ entry during the command seemed comparable to that which enters during the relaxation of $I_{Ca}$ following the command. Finally, signs of $K^+$ accumulation were apparent after even brief depolarization Thus, another aim of the report is to describe some of the complications that can be encountered in attempting to study separately the various $K^+$ currents found in vertebrate neurones.

Parts of this work have appeared previously in abstract form (see Lancaster, Pennefather & Adams, 1985; Pennefather, 1986).

## METHODS

Experiments were performed on paravertebral sympathetic ganglia of the bull-frog *Rana catesbeiana* superfused *in vitro* with various Ringer solutions (see Table 1). Connective tissue surrounding the ganglia was removed as much as possible by dissection and trypsin treatment (1 % (w/v), Sigma grade IV diluted in solution A) for 10 min. Individual ganglia were then pinned onto Sylgard at the bottom of a perfusion chamber. The medium was adjusted to a pH of 7·2 by adding HCl. Blocking agents such as TTX (tetrodotoxin) (1 $\mu$M; Sigma) or $Cd^{2+}$ (200 $\mu$M) were added directly to Ringer solutions. Ganglia were continuously superfused at a rate of approximately 5 ml/min. Experiments were carried out at room temperature.

Voltage-clamp procedures were essentially as described previously (Adams *et al.* 1982*a*; Pennefather *et al.* 1985*b*), with some minor modifications. Micro-electrodes were pulled from 1·5 mm outside diameter 1 mm inside diameter glass tubing with internal filament (Glass Company of America) on an Industrial Science electrode puller. Electrodes were filled with 3 M-KCl and bevelled to a resistance of 10–30 M$\Omega$. Silver paint was applied to both voltage and current electrodes to within 100 $\mu$m of the tip and covering approximately two-thirds of the rest of the electrode. The shank of the electrode was then insulated with a layer of M-coat D (Measurements Group Inc.). The silver-paint shield of the current electrode was grounded, while that of the voltage electrode was connected to a driven shield. A grounded aluminum-foil flag was used to isolate the electrode holders and unpainted portions of the electrodes.

The current electrode was connected either to a WPI M701 amplifier or (in voltage clamp) to the output from the voltage-clamp amplifier, this transition being achieved by a breakaway box. The voltage-clamp current was monitored by a 3 M-KCl agar-bridge bath electrode connected to a virtual-ground circuit. The voltage electrode was connected to a WPI M707 amplifier; the output of this passed to the voltage-clamp amplifier. The voltage-clamp amplifer itself consisted of a Tektronix AM502 differential amplifier (high-frequency 3 dB cut-off at 30 or sometimes 100 kHz) and an operational amplifier (Tektronix AM501). This voltage-clamp system allowed a gain of 10–50000, with 20000 being commonly achieved. The performance of the voltage clamp gave a transition time of 50–100 $\mu$s for large (50 mV or more) voltage excursions and a capacitative current settling time of 100–500 $\mu$s. Clamped cells with settling times greater than 500 $\mu$s were considered unsuitable for the protocols involving large, but brief ($\leqslant$ 3 ms) voltage jumps. The cells used in this study had membrane potentials of at least $-35$ mV after impalement with two electrodes and action potentials greater than 60 mV in amplitude. Cells were greater than 30 $\mu$m in diameter and thus were likely to be B cells (see Dodd & Horn, 1983).

Voltage-clamp records were obtained by taking Polaroid photographs from a storage oscilloscope

(Tektronix 5111) or by read-out onto a chart recorder (Gould 2400) equipped with a wave form digitizing module to produce accurate records of short-duration events. Some data were recorded on tape (Racal 4-DS) for off-line analysis with a Nicolet 1170 signal averager and $X-Y$ plotter (Houston Instruments). All records are displayed as raw data; capacitative and leakage currents have not been subtracted. Records were measured using a ruler or a transparent graph-paper ovelay. Time constants were determined graphically using semilogarithmic paper. Averaged values are expressed in terms of mean $\pm$ S.E. of mean unless otherwise noted.

TABLE 1. Ionic composition of Ringer solution

| Ringer solution | A | B* | C | D* | E | F† |
|---|---|---|---|---|---|---|
| NaCl | 115·0 | 115·0 | — | — | 115·0 | 90 |
| KCl | 2·5 | 2·5 | 40·0 | 40·0 | 2·5 | 25 |
| $CaCl_2$ | 4·0 | — | 4·0 | — | 2·0 | — |
| $MgCl_2$ | — | 4·0 | — | 4·0 | 10·0 | 10·0 |
| Tris‡ | 2·5 | 2·5 | 2·5 | 2·5 | 2·5 | 2·5 |
| Sucrose§ | — | — | 134·0 | 134·0 | — | — |

* 0 $Ca^{2+}$ solutions also contained 0·2 mM-EGTA.
† Solution F also contained 0·2 mM-$Cd^{2+}$ and 1 mM-octanol.
‡ pH = 7·2–7·4.
§ 134 mM-sucrose has the same osmolarity as 77·5 mM-NaCl.

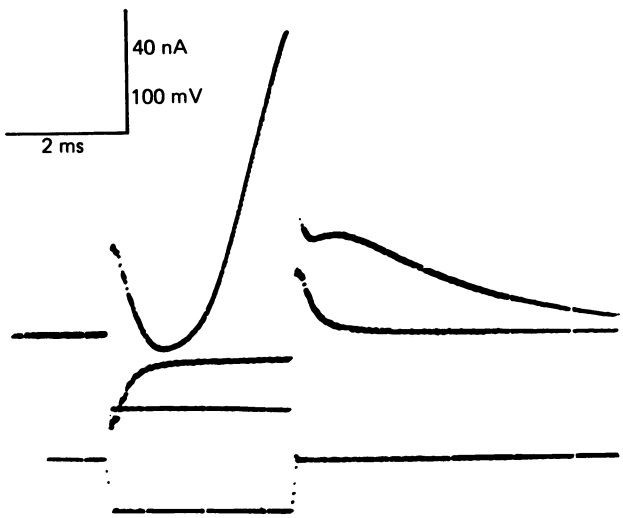


Fig. 1. Currents evoked by 3 ms voltage-clamp commands to 0 and −80 mV. Holding potential −40 mV.

## RESULTS

### *Currents during brief depolarizations: effects of $Ca^{2+}$*

A brief (3 ms) depolarizing voltage-clamp command from −40 to 0 mV evokes an inward current followed by a larger outward current (Fig. 1). Upon return to the holding potential there is an outward tail current that decays rapidly. A brief hyperpolarizing command from −40 to −80 mV does not affect active membrane conductance. The time course of the current evoked by such a command reflects capacity currents which decay within a few hundred microseconds. The magnitude reflects input resistance which in turn is dependent on resting conductances due to

M-channels and leak channels (Adams *et al.* 1982*a*). Since $I_{AHP}$ and $I_M$ are both small with slow time constants at −40 mV, they can be ignored in the treatment of the large, outward currents and corresponding tail currents. TTX or zero $Na^+$ solutions were routinely used to ensure that remote unclamped spikes in the axon did not introduce distortion. In general, however, these treatments had no effect on the amplitude and time course of $K^+$ currents.

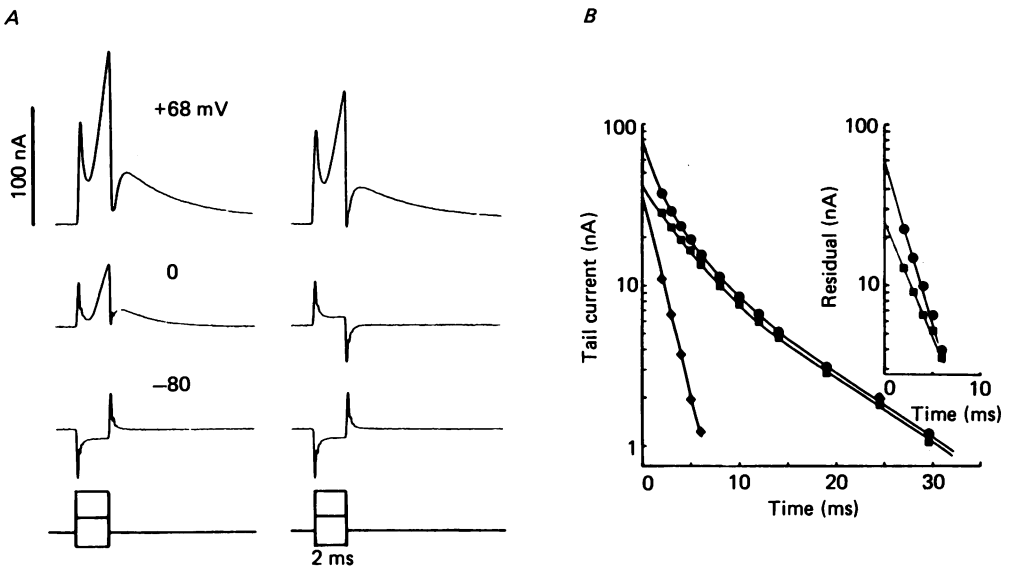


Fig. 2. Effect of $Cd^{2+}$ on currents evoked by brief (2 ms) voltage-clamp commands. All recordings were made in solution A containing TTX (1 μM). *A*, current evoked by commands to +68, 0 and −80 mV. Current on right recorded in the presence of added $Cd^{2+}$ (0·2 mM) to block $Ca^{2+}$ currents. *B*, semilogarithmic plots of tail currents following the commands shown in *A*: ◆, tail current following the command to 0 mV in control solution, following command to 0 mV in the presence of $Cd^{2+}$ outward tail currents were absent; ●, tail current following command to +68 mV in control; ■, tail current following command to +68 mV in the presence of $Cd^{2+}$. $\tau_{fast}$ = 2·2 ms, $\tau_{slow}$ = 10·5 ms. Inset shows residual component of tail current obtained after subtracting slow component; symbols as in *B*, $\tau$ = 2·2 (control) and 3 ms ($Cd^{2+}$). Holding potential −40 mV.

In order to assess the contribution of $I_K$ and $I_C$ to the large outward currents we examined the effect of blockade of $I_{Ca}$; this is illustrated in Fig. 2. In the presence of 1 μM-TTX, where 80 % of the net inward current is abolished, blockade of $I_{Ca}$ with 0·2 mM-$Cd^{2+}$ causes a small additional reduction of net inward current. With a 2 ms command to 0 mV most of the outward current is blocked by $Cd^{2+}$. With commands to +68 mV, $Cd^{2+}$ is less effective. Since the instantaneous conductance of $K^+$ currents is constant in the potential range between −40 and +90 mV (see Adams *et al.* 1982*a*, *c*), the amplitude of $K^+$ tail currents should be directly proportional to the magnitude of $K^+$ currents activated during the command. Semilogarithmic plots of tail currents show that following a command to 0 mV, the tail decays monoexponentially but, following a command to +68 mV, the tail current is biphasic and only the fast component is reduced by $Cd^{2+}$. In addition, the time constant of the tail following

the command to 0 mV was identical to that of the fast component of the tail following the command to +68 mV. Thus, both probably reflect the decay of the same current. The large amplitude, rapid kinetics and $Ca^{2+}$ dependence make it likely that the

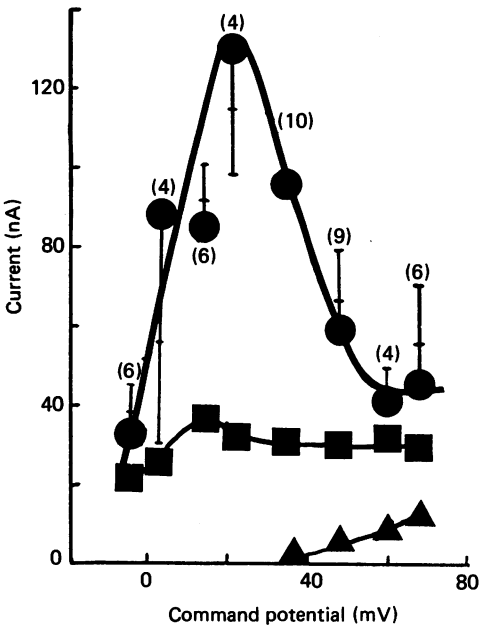


Fig. 3. Averages of currents evoked by 2 ms commands from a series of ten cells. Solution A plus TTX (1 $\mu$M). The amplitudes of the fast and slow components of the tail current determined by extrapolation of those components back to the time when the command potential was terminated were used to estimate $I_C$ (■) and $I_K$ (▲) components respectively. Standard errors for mean values of $I_C$ and $I_K$ are less than the size of the symbols. $I_N$ (●) is the net outward current at the end of the command. Leak current was calculated from the leak current seen with a 2 ms command to −80 mV by assuming a linear relation between leak current and membrane potential. Leak current was subtracted from the peak outward current to obtain $I_N$. Values of $I_N$ were corrected for intercell variability using the ratio $I_N$ at +34 mV/mean $I_N$ at +34 mV as an index of variability (see text). Bars indicate standard error and standard deviation. Values in parentheses indicate number of observations. Lines joining points were drawn by eye. Holding potential was −40 mV.

current is $I_C$ (see Adams *et al.* 1982*c*). The properties of the slow component are consistent with $I_K$ relaxations (Adams *et al.* 1982*a*). Thus the contributions of $I_C$ and $I_K$ can be distinguished from the relative amplitudes of the fast and slow tail currents as well as in terms of $Ca^{2+}$ dependence.

Reduced blockade of the fast component following a command to +68 mV may be due to voltage dependence of blockade by $Cd^{2+}$ or direct activation of $Ca^{2+}$-dependent currents by voltage. In three cells following commands to +68 mV, $Cd^{2+}$ reduced fast tails to 23±9% of control values; tail currents following commands to 0 mV were reduced to less than 5% of control. Fig. 2 illustrates the most $Cd^{2+}$-resistant fast tail we observed; the fast tail was reduced to about 40% of control. A slowing of the residual fast component of the tail current in $Cd^{2+}$ was consistently observed;

in three cells the time constant was $1{\cdot}6 \pm 0{\cdot}2$ times that of control. A further observation with $Cd^{2+}$ was that outward pulse currents during large depolarizing commands were consistently reduced (to $55 \pm 11$ % of control). It is unlikely that the latter effect is due to blockade of $Ca^{2+}$ influx since the $I_{Ca}$ is small at +68 mV (Adams *et al.* 1982*b*). Possibly $Cd^{2+}$ is blocking efflux of $K^+$ through $Ca^{2+}$ channels (see Reuter & Scholz, 1977; Lee & Tsien, 1982; Marty & Neher, 1985).

*Voltage sensitivity of large outward currents*

*Current amplitudes.* Fig. 3 shows the currents evoked by 2 ms voltage-clamp commands. A 2 ms command duration was chosen because the outward current evoked by longer commands was often too large to clamp (i.e. greater than 200–300 nA). Currents of the order of 200 nA could be observed with 2 ms commands to +20 mV. This corresponds to a conductance of about 2 $\mu$S. Thus B cells can increase their conductance approximately 100–200-fold within 2 ms. Net outward current ($I_N$) was determined by subtracting an estimate of the leak current from the total outward current measured at the end of the command. Leak current was extrapolated from the current associated with a hyperpolarizing command to −80 mV from the holding potential of −40 mV (see Fig. 1); the extrapolation assumes that leak current is time independent and non-rectifying (see Adams *et al.* 1982*a*).

The magnitude of $I_N$ produced by a given command was quite variable from cell to cell. Presumably this reflects variations in cell size and perhaps the extent to which $I_{Ca}$ survives impalement of the cell with micro-electrodes. We attempted to deal with the variability by dividing all values of $I_N$ recorded in a given cell by the value of $I_N$ associated with +34 mV command, then multiplying the resultant by the mean value of $I_N$ at +34 mV ($95 \pm 19$ nA, $n = 10$). The remaining variability possibly reflects the rather steep slope of the current–voltage relation on either side of the peak that occurs at +20 mV. Values of $I_C$ and $I_K$ derived from tail currents proved to be much less variable and were simply averaged.

A clear negative-slope region was apparent between +20 and +60 mV. This is conventionally attributed to a reduction in the $Ca^{2+}$-dependent outward current which is secondary to a reduced inward $Ca^{2+}$ current as the command potential approaches $E_{Ca}$ ($Ca^{2+}$ reversal potential) (Meech & Standen, 1975). The peak of the $Ca^{2+}$-dependent outward current is maximal at about +20 mV which is also consistent with the activation curve for $Ca^{2+}$ currents, in this preparation and others, showing them to be maximal in this region (Akaike, Lee & Brown, 1978; Adams *et al.* 1982*b*; Hagiwara & Ohmori, 1982; Fenwick, Marty & Neher, 1982). At membrane potentials above +60 mV, the electrochemical gradient for $Ca^{2+}$ will be such that $Ca^{2+}$ influx will be much smaller than at +20 mV. Paradoxically, after commands to these potentials, tail-currents continue to display a fast component with a time constant and $Ca^{2+}$ sensitivity identical to the $I_C$ component with 2 ms commands, the $I_C$ component is reduced by less than 2-fold as command potentials approach the reversal potential for $I_{Ca}$.

The $I_C$ component of $K^+$ tail currents following commands positive to +60 mV may be generated by a $Ca^{2+}$ tail current that flows upon repolarization to the holding potential. In B cells $I_{Ca}$ exhibits exponential turn-on and turn-off kinetics. The time

constant is slowest at 0 mV (5 ms) and accelerates on either side reaching less than 1 ms at +40 mV. Between −40 and +40 mV, the instantaneous current–voltage relation is linear with an extrapolated reversal potential at around +60 mV (Adams *et al.* 1982*b*; P. R. Adams, unpublished observation). Using these values one can calculate that for 2 ms commands, the tail current will contribute 80 % of total $Ca^{2+}$

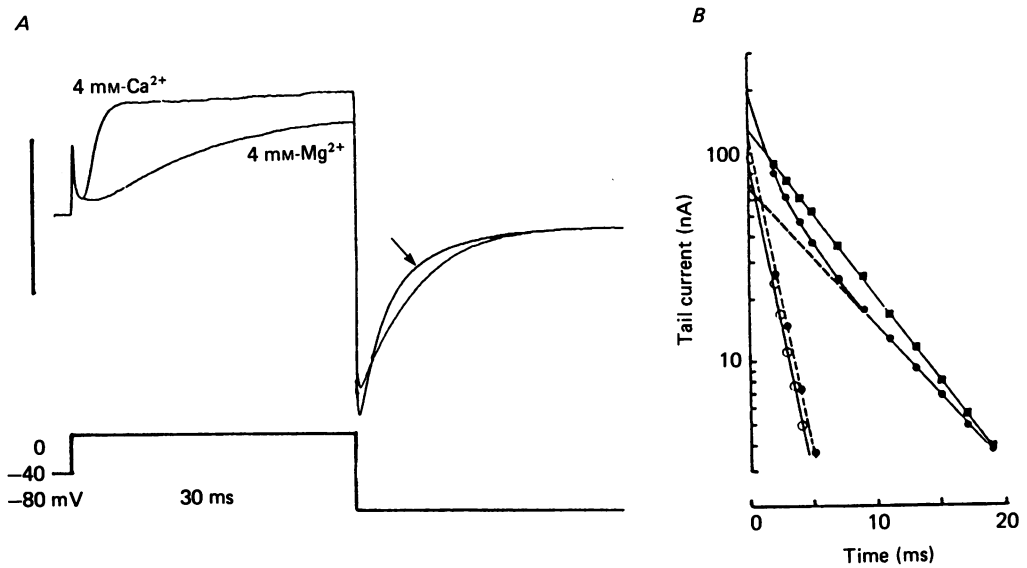


Fig. 4. Effect of replacing $Ca^{2+}$ with $Mg^{2+}$ on $K^+$ currents. Solutions contained zero $Na^+$, 40 mM-$K^+$, 100 mM-sucrose, and either 4 mM-$Ca^{2+}$ or 4 mM-$Mg^{2+}$ + 0·2 mM-EGTA (solutions C and D). $K^+$ currents were evoked by a 30 ms command to 0 mV. Tail currents were measured at −80 mV to increase the driving force. *A*, superimposed records of currents in the two solutions. Arrow indicates current in 4 mM-$Ca^{2+}$. *B*, semilogarithmic plots of tail currents at −80 mV. In 4 mM-$Mg^{2+}$ (■) the tail current is monophasic ($\tau$ = 18·5 ms) while in 4 mM-$Ca^{2+}$ (●) the tail current is biphasic ($\tau_{fast}$ = 3·1 ms, $\tau_{slow}$ = 22·6 ms). The residual (●---●) left after subtracting the slow component of the tail in 4 mM-$Ca^{2+}$ has the same time constant as the tail current following a ·2 ms pulse to 0 mV in the same cell (○). Holding potential was −40 mV.

entry associated with commands to +40 mV and 60 % associated with commands to 0 mV. In 4 mM-$Ca^{2+}$ approximately 4 pC of $Ca^{2+}$ will enter during a tail current at −40 mV following maximal activation of $I_{Ca}$ (P. R. Adams, unpublished observation).

A slow component in the $K^+$ tail current following 2 ms pulses was evoked only by commands to +34 mV or greater. In this series of cells the slow component ($I_K$) of the tail current at −40 mV had a time constant of 21·3 ± 3·2 ms, and the time constant of the fast component ($I_C$) was 2·4 ± 0·3 ms. Both time constants were independent of the command potential. These values are similar to those reported by Adams *et al.* (1982*a*, *c*) for tail currents following longer voltage-clamp commands. The absolute values of the time constants varied somewhat from experiment to experiment, possibly because temperature was not controlled (room temperature varied between 18 and 28 °C depending on the season). However, in all cases the time constant of the two components differed from one another by an order of magnitude.

*Rate of opening.* In order to study the rate at which $I_C$ and $I_K$ are activated, it is necessary to separate the contributions of the two currents to the total outward currents. One of the complications involved in assessing the contribution of $I_K$ and $I_C$ to total outward current is that there is no specific agent to block $I_K$ and leave $I_C$ unaffected. However $I_K$, unlike $I_C$, is not dependent on $Ca^{2+}$ influx. It should therefore be possible to prevent activation of $I_C$ in zero-$Ca^{2+}$ medium. Indeed, Adams *et al.* (1982*a*) used this method to study the voltage dependence of $I_K$ activation. It should also be possible to define the time course of activation of $I_C$ in terms of the difference current defined by the $Ca^{2+}$-dependent portion of the outward current. The voltage dependence of $I_C$ activation is expected to be rather complex. The perturbation in $I_C$ kinetics introduced by the voltage clamp is not a simple function of voltage; it depends also on the kinetics of $I_{Ca}$ and intracellular $Ca^{2+}$ concentration ($[Ca^{2+}]_i$). Despite these anticipated problems we expected that an empirical description would be possible.

Fig. 4 shows the results of replacing $Ca^{2+}$ with $Mg^{2+}$ in the Ringer solution. These experiments were carried out in a zero-$Na^+$, raised-$K^+$ medium (solutions C and D). Adams *et al.* (1982*a*) have shown that $K^+$ accumulation in the restricted extracellular spaces surrounding ganglion cells can severely distort outward currents evoked by voltage-clamp commands. Hence, raised $K^+$ was used to reduce the influence of accumulation of $K^+$ in extracellular spaces that might accompany increases in $K^+$ currents. Replacement of $Na^+$ by isotonic sucrose had no effect on the magnitude or time course of $K^+$ currents and produced a more complete block of $Na^+$ currents than did 1 $\mu$M-TTX. The other major time-dependent inward current found in these cells, $I_{Ca}$, is only a few nanoamperes (Adams *et al.* 1982*c*). Thus, the modified media minimized as much as possible distortions of the rising phase of outward currents.

In 40 mM-$K^+$ (solutions C and D) $K^+$ currents are inward at $-40$ mV. In solution C which contained $Ca^{2+}$, a 30 ms command to 0 mV evoked a tail current that decayed with two exponentials (Fig. 4). The faster component had a time constant identical to that of the monoexponential tail that follows a brief 3 ms pulse (Fig. 4*B*) and is thus most likely an $I_C$ tail current. When $Ca^{2+}$ is replaced by $Mg^{2+}$ (solution D) the remaining pulse current develops only after a significant delay. This delay is a characteristic of $I_K$ (see Adams *et al.* 1982*a*) and explains the lack of a slower component of tail currents following brief commands to 0 mV. In solution D, the $K^+$ tail current lacks a fast component and represents the monoexponential relaxation of $I_K$ alone (Fig. 4*B*).

A cursory examination of Fig. 4 suggests that the $Ca^{2+}$-dependent component of outward current (i.e. $I_C$) has a transient component. However, a closer examination indicates that $I_K$ has also been changed by switching from solution C to solution D. The slow tail recorded in the absence of $Ca^{2+}$ (solution D) is larger and slightly briefer than that recorded in the presence of $Ca^{2+}$ (solution C). This suggests that in addition to preventing the activation of $I_C$, replacement of $Ca^{2+}$ with $Mg^{2+}$ also affects $I_K$ (see also Armstrong & Matteson, 1986).

In media containing 40 mM-$K^+$ and 0 $Na^+$, the rate of opening of $I_K$ was increased, further complicating attempts to study the activation kinetics of $I_K$ and $I_C$ separately. Our evidence for this effect comes from comparison of current–voltage relations in solution A and solution C. Fig. 5 shows the current–voltage relation recorded from a cell where it proved possible to study a wide range of 2 ms commands before, during

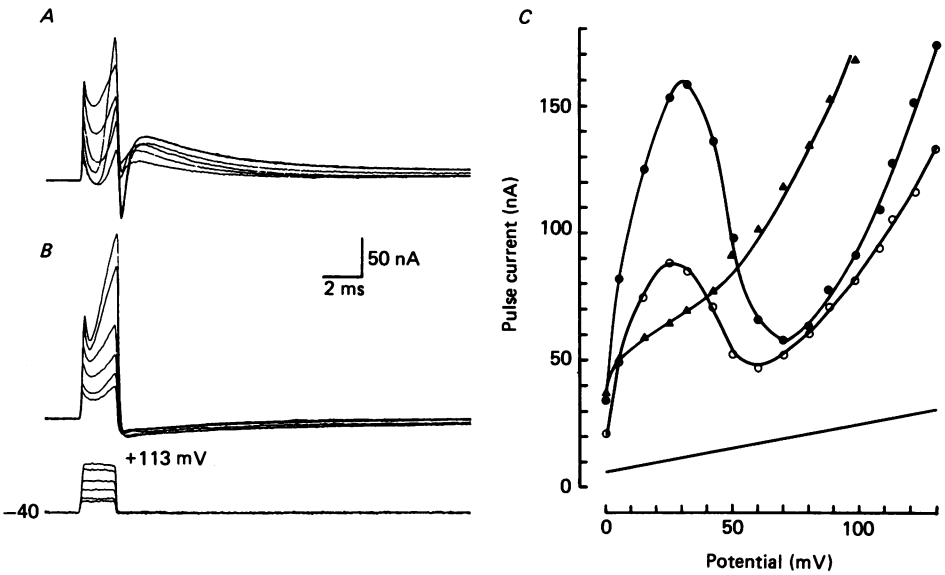


Fig. 5. Effect of raised $K^+$ on the relation between the command potential and outward currents evoked by 2 ms commands. *A*, series of responses to increasing commands in control solution (solution A). *B*, response to the same series of commands in solutions containing 40 mM-$K^+$ and 0 $Na^+$ (solution C). *C*, current–voltage relation, pulse current at the end of 2 ms commands is plotted against command potential; ●, solution A; ▲, solution C; ○, recontrol in solution A. Straight line at the bottom of the Figure represents the leak current estimated from the current resulting from a 2 ms command to −80 mV, $\tau_{fast}$ = 4 ms, $\tau_{slow}$ = 19 ms. Holding potential was −40 mV.

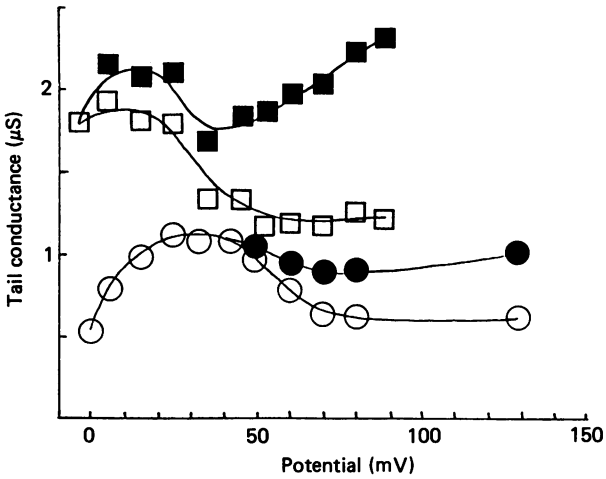


Fig. 6. Relation between command potential and tail conductance following a 2 ms command. Tail currents were measured in solution A (circles) and solution C (squares). Tail conductance was calculated by dividing tail-current amplitude by driving force; $E_K$ was estimated to be −106 mV in solution A and −31 mV in solution C (see text and Table 2). Open symbols represent the amplitude of the fast component ($I_C$) of tails, filled symbols are the total amplitude of tails. Difference between open and filled symbols represents conductance due to $I_K$. Data from same cell as in Fig. 5. Holding potential −40 mV.

and after exposure to solution C (40 mM-$K^+$). There may have been some run-down of $Ca^{2+}$ current over the course of the experiment accounting for the incomplete recovery of outward currents upon return to control media (Fig. 5*C*). Nevertheless the results are clear and typical of what was observed in other cells. Outward currents produced by commands to around +20 mV are smaller in solution C, as expected

TABLE 2. Instantaneous reversal potential for $K^+$ current calculated from the data described in Figs. 6 and 7

| Solution | $V$ (mV) | $I_K$ (nA) | $I_C$ (nA) | $I_T$ (nA) | $I_T^*$ (nA) | $I_N$ (nA) | $E_K$ (mV) |
|---|---|---|---|---|---|---|---|
| A, 2.5 mM-$K^+$ | 42 | 1 | 65 | 66 | 28 | 126 | (−62) |
| | 50 | 6 | 59 | 65 | 27 | 87 | (−83) |
| | 60 | 11 | 47 | 58 | 20 | 53 | (−92) |
| | 70 | 16 | 38 | 54 | 16 | 43 | −106 |
| | 80 | 18 | 38 | 56 | 18 | 50 | −107 |
| C, 40 mM-$K^+$ | 45 | −4 | −11 | −15 | −5 | 50 | −32 |
| | 52 | −5 | −10 | −15 | −5 | 64 | −33 |
| | 60 | −6 | −10 | −16 | −6 | 71 | −32 |
| | 70 | −7 | −9 | −16 | −6 | 82 | −32 |
| | 77 | −8 | −10 | −18 | −8 | 97 | −31 |
| | 88 | −9 | −10 | −19 | −9 | 110 | −28 |

$E_K$ was estimated on the assumption that the $K^+$ conductance at the end of a command to a potential ($V$) equalled that at the holding potential ($V_h$) immediately after the command provided the tail conductance was corrected for the component of $I_C$ generated by a tail current. Thus, $I_N (V-E_K) = I_T^* (V_h-E_K)$. Where $I_T^*$ is the tail current ($I_T$) subtracted by the $I_C$ component of the tail current following a command to above +80 mV. The relation assumes that the instantaneous current–voltage relation of $K^+$ currents is linear in the potential range studied (−40 to +90 mV) and that following 2 ms command to +40 mV or greater a constant amount of $Ca^{2+}$ enters during the $Ca^{2+}$ tail current and contributes to the generation of the $I_C$ component of $I_T$. Bracketed results are likely to be over-estimates (see text).

from the reduced driving force. However with commands to +50 mV and above, outward currents are larger. As a result, the negative slope region is obscured. As mentioned above, the negative-slope region of the current–voltage relation is thought to reflect reduced entry of $Ca^{2+}$ and hence reduced activation of $I_C$ as command potentials approach the reversal potential of $Ca^{2+}$ currents. Outward currents produced by commands above +50 mV reflect primarily $I_K$, suggesting that brief commands activate proportionally more $I_K$ in solutions containing elevated levels of $K^+$ (see also Dubois, 1981).

Increased activation of $I_K$ in solution C was confirmed by examination of tail currents. Fig. 6 plots the conductance of $K^+$ currents associated with the pulse currents of Fig. 5. Tail conductance is simply the product of the tail-current amplitude and the difference between −40 mV and $E_K$ ($K^+$ reversal potential). For solution C, $E_K$ was set at −31 mV and for solution A, $E_K$ was set at −106 mV (see Table 2). In 40 mM-$K^+$ tail conductance was twice that in 2·5 mM-$K^+$. Constant-field rectification predicts a 3-fold increase (see Hodgkin & Katz, 1949) but with this cell, outward currents did not completely recover upon return to control media.

$I_K$ components are apparent in tail currents following 2 ms commands that are more positive than 0 mV rather than +30 mV as is the case in medium containing

2·5 mM-$K^+$. This implies that in raised $K^+$, the negative-slope region is obscured because the growing contribution of $I_K$ to the total outward pulse current during successively larger voltage-clamp commands is able to offset the decline in $I_C$ that occurs as $I_{Ca}$ is reduced.

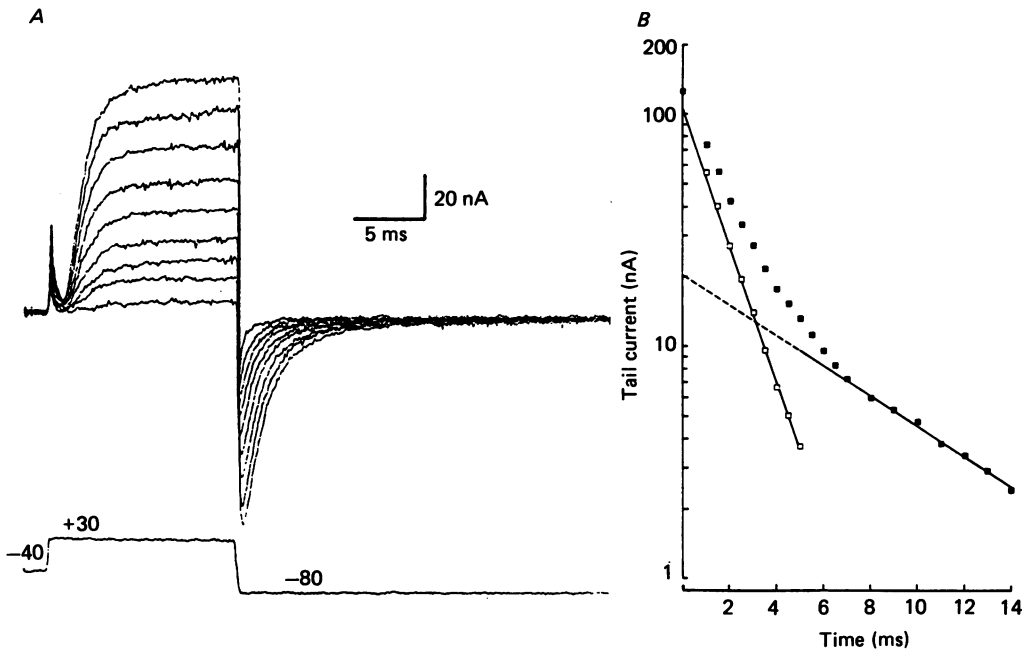


Fig. 7. Outward current evoked by 13 ms commands in raised $K^+$, 0 $Na^+$ (solution B). *A*, outward currents evoked by commands, successively incrementing in 5 mV steps, to between −10 and +30 mV followed by a post-pulse command to −80 mV, holding potential is −40 mV. *B*, semilogarithmic plot of tail current (■) and fast component residual (□) at −80 mV following the command to +30 mV and shown in *A*. $\tau_{fast}$ = 1·5 ms, $\tau_{slow}$ = 7 ms.

In contrast to $I_N$, the $I_C$ component of the corresponding tail current shows a much smaller decline as command potentials approach the reversal potential for $Ca^{2+}$ currents. In addition, the amplitude of the fast component of the tail conductance is similar following all commands above +60 mV. This is what would be predicted if $Ca^{2+}$ entry via an $I_{Ca}$ tail current was sufficient to activate $I_C$ (see above). Since $I_{Ca}$ can be mostly activated by the end of 2 ms commands to +40 mV or more (see Adams *et al.* 1982*b*) a similar $Ca^{2+}$ tail current must contribute to the generation of the $I_C$ component of the $K^+$ tail current following all commands greater than +40 mV. Indeed, the calculated instantaneous $K^+$ reversal potential only agrees with the demonstrated reversal potential if the amplitude of the tail current is first corrected ($I_T$*) by subtracting the limiting fast component of the tail current following the command to around +80 mV (Table 2). This approach, applied to the data used in Figs. 5 and 6, predicted values for $E_K$ close to −30 mV for solution C and −100 mV for solution A. Both values agree with directly observed values (Fig. 9; Pennefather *et al.* 1985*b*) and predict an intracellular $K^+$ concentration of around 140 mM (from the Nernst equation).

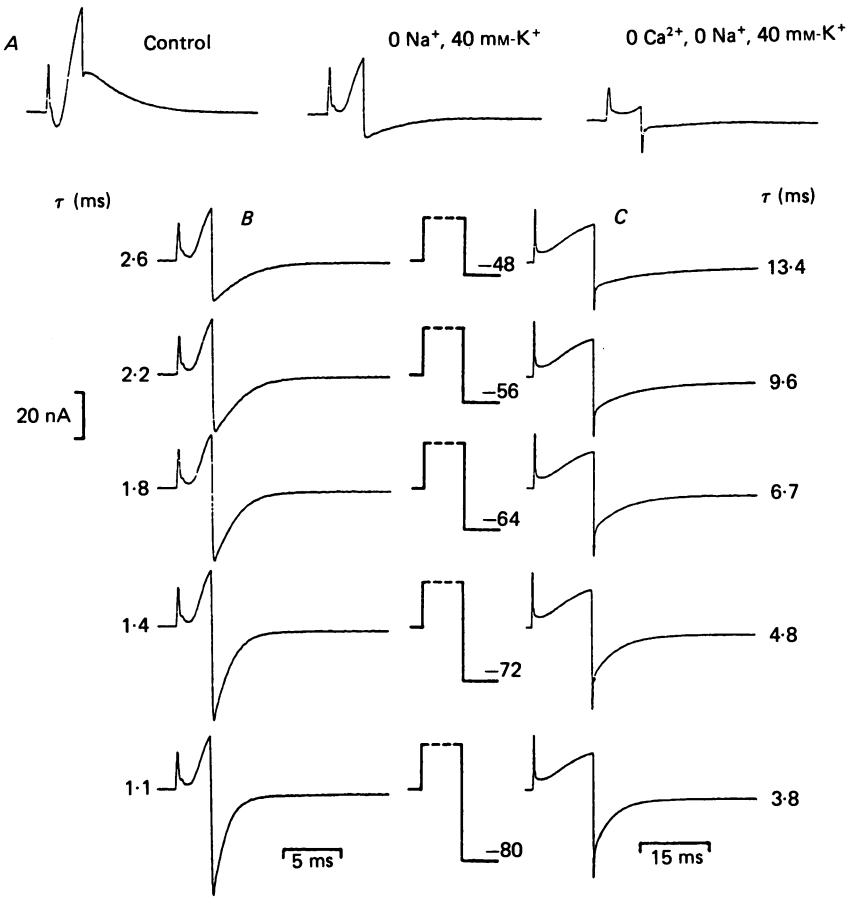


Fig. 8. Protocol for determining the voltage sensitivity of $I_C$ and $I_K$ tail currents. *A*, currents evoked by 3 ms commands to 0 mV from a holding potential of −40 mV in three different solutions: solution A, solution C (0 $Na^+$, 40 mM-$K^+$) and solution D (0 $Ca^{2+}$ 0 $Na^+$, 40 mM-$K^+$). When 40 mM-$K^+$ is present the 3 ms depolarizing command is followed immediately by a post-pulse command to −80 mV in order to increase the size of the tail current. *B*, currents following 3 ms commands at different potentials in solution B. Time constant of the tail current is indicated on the left. Post-pulse potential is indicated in the middle. *C*, currents following 13 ms commands in solution D. Tail-current time constants indicated on the right. For each row, the post-pulse potential is the same as in *B*.

In solution A (2·5 mM-$K^+$) the calculations only generate a reasonable value for $E_K$ when $I_N$ was small. Larger currents appeared to be associated with significant accumulation of $K^+$ within 2 ms, so that more positive values of $E_K$ were calculated. These values are presented in brackets because they must be over-estimates. A major assumption in the calculation presented in Table 2 is that $E_K$ remains constant. If extracellular $K^+$ increases as a result of the outward current, the calculated $E_K$ will be more positive than the actual $E_K$. Although these calculations provide an indication that $K^+$ accumulation can occur with brief commands, they do not allow the magnitude of the accumulation to be quantified.

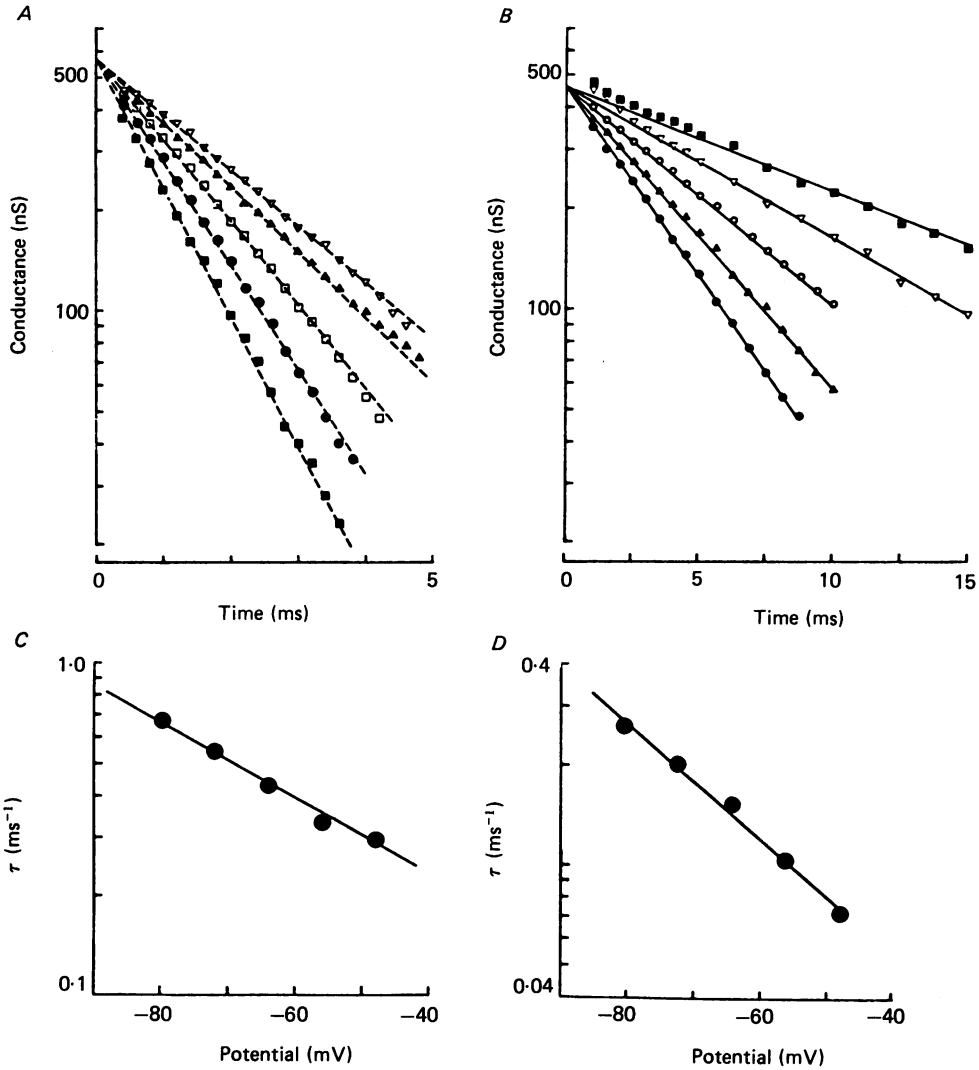


Fig. 9. Voltage sensitivity of $I_C$ and $I_K$ tail currents. $E_K$ was determined from a plot of tail current amplitude *vs.* post-pulse potential and used to convert tail currents to conductances. *B* and *D* from the data in Fig. 8; *A* and *C* from a different cell. *A*, semilogarithmic plots of $I_C$ tail conductances at different post-potentials following 3 ms commands in solution C (see Fig. 8); $E_K = -30$ mV. *B*, semilogarithmic plots of $I_K$ tail conductances at different post-potentials following 13 ms commands in solution D; $E_K = -25$ mV. *C*, semilogarithmic plot of $I_C$ time constant *vs.* post-potential; line shows $I_C$ tail-current decay rate changes e-fold in 39 mV. *D*, semilogarithmic plot of $I_K$ time constant *vs.* post-potential; line shows $I_K$ tail-current decay rate changes e-fold in 24 mV.

It should be apparent by now that there are many problems in separating the contribution of $I_C$ and $I_K$ to the pulse current. Nevertheless, it is clear that $I_K$ remains a minor component of the outward current evoked by commands to +30 mV or below, even in 40 mM-$K^+$. Fig. 7 shows that only 18% of the tail current following

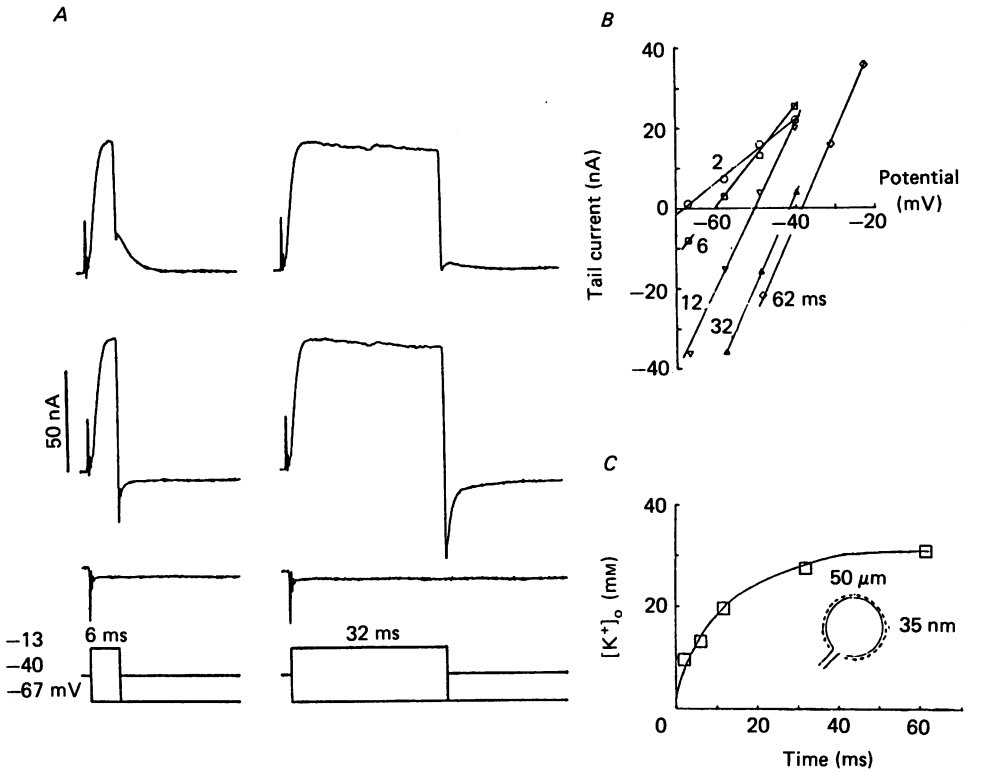


Fig. 10. Effect of $K^+$ current duration on $E_K$. $E_K$ is determined by measuring the amplitude of tail currents at different post-pulse potentials following commands of different durations to −13 mV; holding potential −40 mV, solution A with added TTX (1 μM). *A*, examples of data. *B*, plots of tail-current amplitude *vs.* post-pulse command potential for pulses of different duration (shown in milliseconds). *C*, reversal potential is converted to concentration of $K^+$ outside the cell ($[K^+]_o$) from Nernst equation assuming intracellular $K^+$ = 140 mM; $[K^+]_o$ is plotted *vs.* pulse duration. Time constant of accumulation is 14 ms. Inset, schematic diagram of restricted space assuming cell is spherical with a diameter of 50 μm and that the space is of uniform width (35 nm) over the entire surface of the cell.

a 13 ms command to +30 mV is $I_K$. For commands to potentials less than +30 mV the contribution of $I_K$ is less. With long commands $Ca^{2+}$ entry during the $Ca^{2+}$ tail current makes less of an impact on total $Ca^{2+}$ influx and the fast and slow components of the tail current more closely reflects the contribution of $I_C$ and $I_K$ to the pulse current. Indeed the instantaneous $K^+$ reversal potential calculated using the actual tail current gives a value close to the demonstrated reversal potential.

Although the outward currents illustrated in Fig. 7 are made up primarily of $I_C$, all we can say about the activation of $I_C$ is that in the range of potential between 0 and +30 mV, it approaches a steady value within 5 ms (Fig. 7). The delay in onset of $I_C$ may be more apparent than real. A number of factors make it difficult to measure the variable; these include, inward currents, the finite time required for the build-up of $[Ca^{2+}]_i$ and the decay of membrane capacitative currents.

*Rate of closing.* The increased $K^+$ conductance activated during an action potential

drives the membrane potential to between −50 and −100 mV which in turn reverses the processes that activated the $K^+$ conductance in the first place. Since deactivation is not instantaneous, there is a period of time during which the membrane potential is negative to rest. This is referred to as the after-hyperpolarization phase of the action potential or a.h.p. It was of interest, therefore, to measure the rate of decay of the tail currents in the range of potentials where $K^+$ currents normally decay. Solution C proved useful for this purpose because the reversal potential for $K^+$ is at −30 mV so that tail currents are larger and easier to measure in the a.h.p. range of potentials than they would be at normal $K^+$ levels. Also problems due to $K^+$ accumulation are minimized.

Fig. 8*A* shows that the kinetics of $I_C$ are not affected by removing $Na^+$ and raising $K^+$. As in the control solution a 3 ms command to 0 mV activates a current that is $Ca^{2+}$ dependent and is associated with a tail current having the same time constant. In order to determine the voltage sensitivity of $I_C$ tail currents, they were measured at various post-pulse potentials following the 3 ms command (Fig. 8*B*). $I_C$ tail currents are plotted in Fig. 9*A*. The time constant of the tail currents changes e-fold per 39 mV (Fig. 9*C*).

After $Ca^{2+}$ has been removed from the medium, the currents elicited by a 3 ms voltage command to 0 mV are virtually eliminated (Fig. 8*A*). However, $I_K$ is activated with commands of 13 ms duration (Fig. 8*C*; Adams *et al.* 1982*a*). The $I_K$ tail currents are plotted in Fig. 9*B*; they show an e-fold change in time constant per 24 mV in the membrane potential range between −80 and −50 mV (Fig. 9*D*).

*$K^+$ accumulation*

Rather than attempting to reduce the influence of $K^+$ accumulation, an alternate approach to dealing with it is to measure the degree of accumulation directly and convert currents into chord conductances. Fig. 10 shows how the time course of $K^+$ accumulation can be estimated by direct determination of $E_K$ at various times after a test command. It is apparent from Fig. 10*A* that following a 6 ms command to −15 mV, $E_K$ was around −67 mV but, if the command was extended to 32 ms, $E_K$ was around −40 mV. Fig. 10*B* plots the tail-current amplitude at different post-potentials following commands of different duration. The reversal potential increased with command duration and appeared to approach a maximum after a pulse of 62 ms. It is notable that the slope conductance increased with command durations up to 12 ms even though the outward current reached a maximum before 6 ms. This indicates that the number of activated channels is increasing during a period that outward current is getting smaller.

In Fig. 10*C* the reversal potentials have been converted into levels of extracellular $K^+$ by assuming that intracellular $K^+$ is equal to 140 mM (see above) and using the Nernst equation. Extracellular $K^+$ appears to accumulate with a time constant of about 14 ms.

The data can be used to calculate the volume of the restricted extracellular space. The rate of $K^+$ accumulation in that space will equal

$$I_N/(F \text{ vol.}),$$

where $I_N$ is the outward current minus the leak current, $F$ is Faraday's number and vol. is the

volume of the restricted space. For a constant $I_N$, the rate constant for $K^+$ accumulation ($k$) will equal the rate constant of $K^+$ loss from the space. If $[K^+]_o$ is the concentration of $K^+$ in the space at time 0 and $[K^+]_{s.s.}$ the concentration at a steady state then,

$$([K^+]_{s.s.} - [K^+]_o)\, k = I_N/(F \text{ vol.})$$

$$\therefore \text{vol.} = I_N/[F\, k([K^+]_{s.s.} - [K^+]_o)].$$

In the case illustrated in Fig. 10, $I_N = 55$ nA, $k = 14$ ms and $[K^+]_{s.s.} - [K^+]_o = 29$ mM, so that volume = 265 $\mu m^3$.

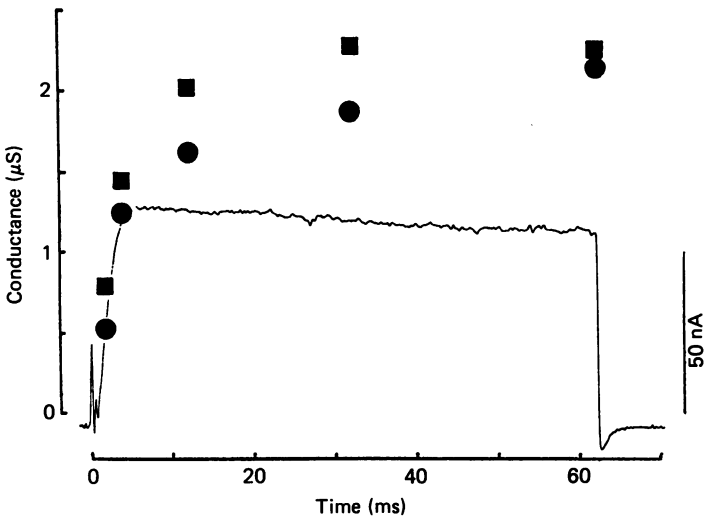


Fig. 11. Time course of $K^+$ conductance compared to $K^+$ current. Same cell and conditions as in Fig. 10. Trace is record of current evoked by a 62 ms command to −13 mV from a holding potential of −40 mV. Circles are conductance calculated from net current at the indicated time divided by the driving force at that time (see Fig. 10*B*). Squares are conductance calculated from the slope of tail current amplitudes *vs.* post-pulse potential.

Although the size of this particular cell was not measured, it is likely to be spherical with a diameter of 50 $\mu m$ (see Adams *et al.* 1982*a*; Dodd & Horn, 1983) and a surface area of 7000 $\mu m^2$. If the restricted space were evenly distributed over such a cell it would have a width of 35 nm. In one other cell where this type of analysis proved feasible, the time constant of accumulation was 21 ms and the estimated volume of the space was 259 $\mu m^3$.

These values must be presented with two caveats. First, the degree of $K^+$ accumulation which we have observed varies widely from cell to cell within a ganglion. The second point is that the values arrived at pertain to a surface ganglion cell (since impalement was under visual control) after dissection and trypsin treatment. It is quite possible that $K^+$ accumulation is even more pronounced *in situ*.

Once the time course of $K^+$ accumulation is known one can assess how it distorts the time course of outward currents. Fig. 11 shows the current produced by a 62 ms command to −13 mV; note the inward tail current upon return to −40 mV. The symbols represent values of conductance calculated in two different manners. Circles represent conductance calculated by dividing the current at a given time by the driving force at that time, while squares represent conductance calculated from the slope of the line relating the amplitude of tail currents at different post-potentials

to membrane potentials. The fact that the latter estimate is greater is consistent with the possibility that $Ca^{2+}$ tail currents increase the $I_C$ component of the $K^+$ tail currents (see above). Regardless of which method is used to determine the conductance, it is apparent that $K^+$ accumulation can lead to a sag in the outward current independent of any decrease in conductance.

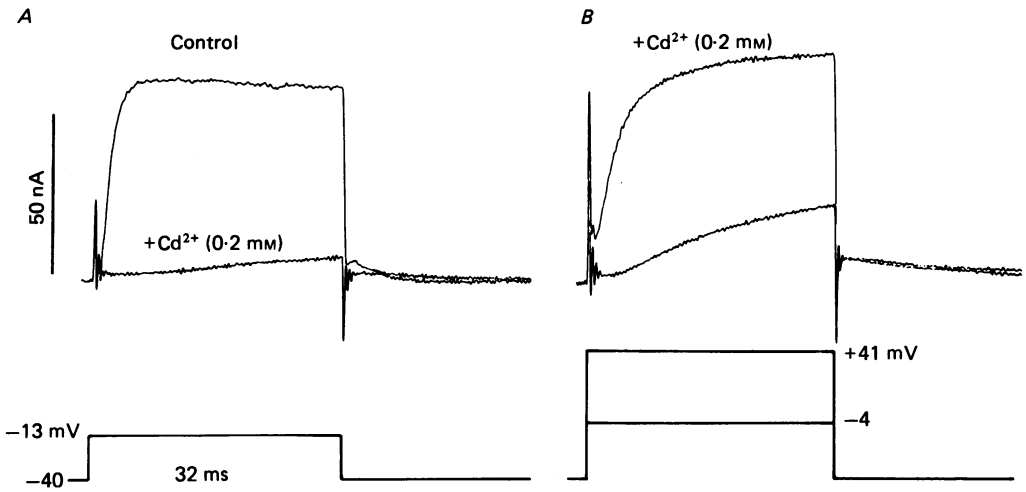


Fig. 12. $K^+$ accumulation is independent of type of $K^+$ current. Holding potential was −40 mV, in solution A. *A*, 32 ms command to −13 mV produced more than 50 nA of outward current that is predominantly $I_C$ since most is blocked by 0·2 mM-$Cd^{2+}$. *B*, in the presence of 0·2 mM-$Cd^{2+}$ larger commands to −4 and +41 mV evoke outward current consisting mostly of $I_K$.

Fig. 12 shows that most of the current flowing during the command to −13 mV is $I_C$; 0·2 mM-$Cd^{2+}$ blocks most of the outward current. Since there are no $Ca^{2+}$ tail currents in $Cd^{2+}$, the instantaneous reversal potentials can be calculated directly from the current at the end of the command and the tail current. In $Cd^{2+}$, at the end of the 32 ms command to −13 mV, $E_K$ was −94 mV. Fig. 12*B* shows outward currents from the same cell, evoked in the presence of 0·2 mM-$Cd^{2+}$ by commands to −4 and +41 mV. $E_K$ was −63 mV after the command to −4 mV and −40 mV after the command to +41 mV. The calculated values for the instantaneous reversal potential values correspond to those determined directly from the reversal potential of the tail current.

It is apparent from Fig. 12 that the delay before $I_K$ develops becomes progressively smaller with more positive voltage-clamp commands; the delay is around 6 ms at −13 mV, 4 ms at −4 mV and less than 1 ms at +41 mV. The delay reflects the characteristic gating properties of $I_K$. However, $K^+$ accumulation must distort the time course to a certain extent, not only as the result of shifts in driving force but also because of direct effects of $K^+$ on the kinetics of $I_K$ (see Fig. 6; Dubois, 1981).

### $I_{AHP}$

We have not yet been able to study carefully the activation of $I_{AHP}$. This current is quite labile and is frequently absent in cells that have been impaled with two

electrodes. Nevertheless, we were able in a few cells, to record an $I_{AHP}$ very similar to that observed using the less traumatic, single-electrode hybrid clamp (see Pennefather *et al.* 1985*b*). We were able to obtain preliminary data concerning the relation between $I_{AHP}$ and command duration and amplitude. As befits a current which is responsible for the slow component of the a.h.p. following a single action

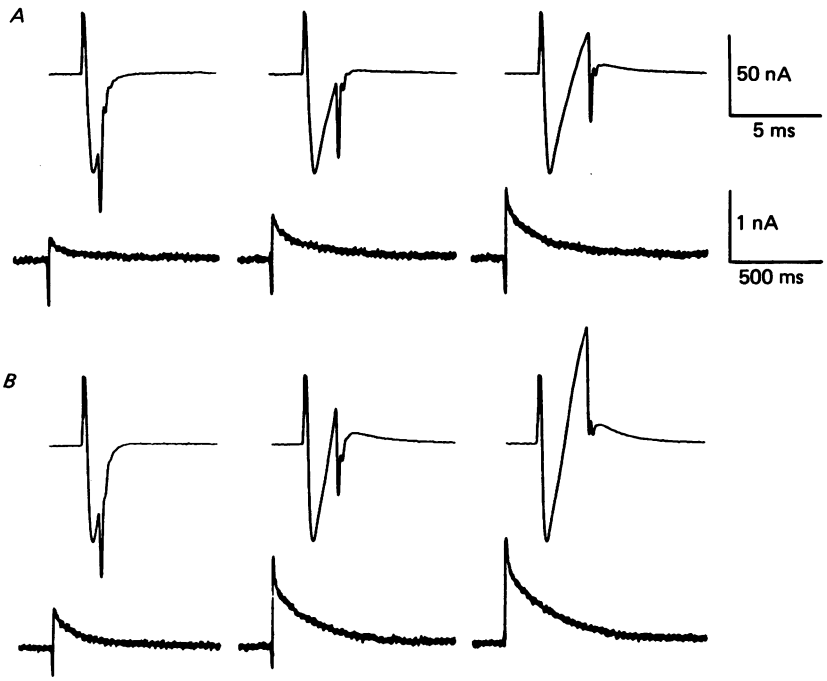


Fig. 13. Time and voltage dependence of $I_C$ and $I_{AHP}$. Both sections show current evoked by, from left to right, 1, 2 and 3 ms commands to 0 mV (*A*) and +10 mV (*B*). Holding potential was −40 mV. Upper traces are fast, low-gain records dominated by inward $Na^+$ current followed by outward $I_C$. Lower traces are the corresponding slow, high-gain records dominated by $I_{AHP}$.

potential, $I_{AHP}$ can be activated by voltage steps as brief as 1 ms in duration (Fig. 13). Following 3 ms commands to 0 mV, the $I_C$ tail currents are in the range of two orders of magnitude larger and faster than $I_{AHP}$ (holding potential −40 mV). We have observed that the total amount of $I_{AHP}$ which is available to be activated is very restricted and appears to reach a saturating peak tail current value of about 1–2 nA (see also Pennefather *et al.* 1985*b*).

Figs. 14 and 15 show data from a cell where a 2 ms command was varied in 10 mV steps between −7 and +63 mV, 3 mM-TEA was added to solution A in order to improve the voltage control at positive potentials. This concentration inhibits more than 75% of $I_C$ and $I_K$ with little effect on $I_{AHP}$ (see Pennefather *et al.* 1985*a*). Although the conductance during the pulse first increased and then decreased as the command potential approaches the $Ca^{2+}$ reversal potential, both $I_C$ and $I_{AHP}$ tail currents following these pulses were relatively constant. These observations suggest that components of both $I_C$ and $I_{AHP}$ tail currents are generated by $Ca^{2+}$ tail currents

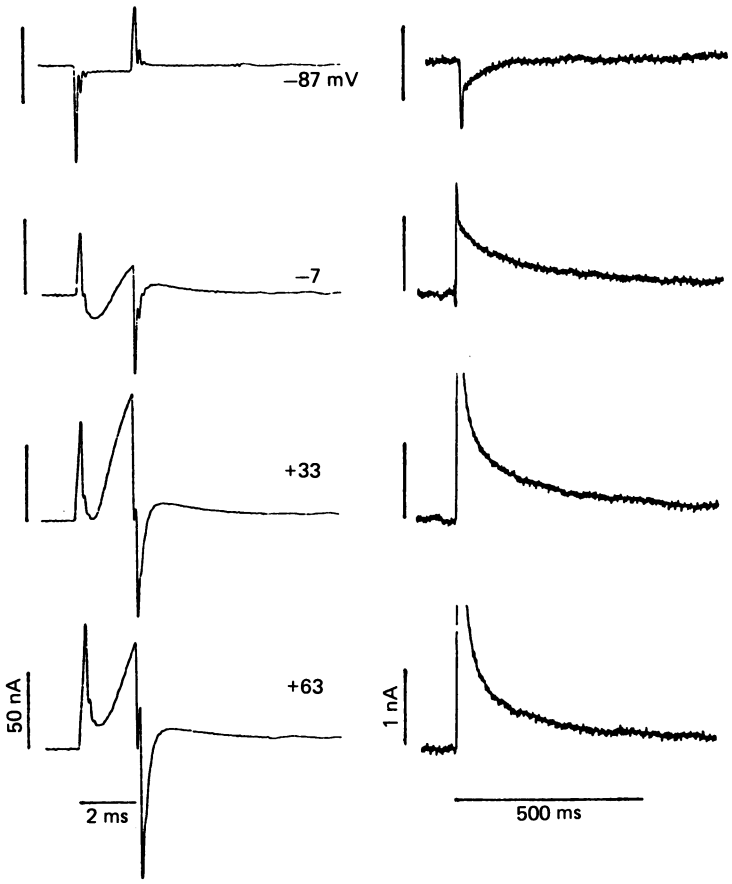


Fig. 14. Tail currents following 2 ms commands in a cell with a prominent $I_{AHP}$. Low gain, fast records in left column, the equivalent high gain, slow records in right column. Holding potential −40 mV, solution A plus 3 mM-TEA, command potential indicated in centre of each row. Tail currents in low gain, fast records are dominated by $I_C$. In high gain, slow records they are dominated by $I_K$ and $I_{AHP}$. Slow relaxation following the command to −87 mV is probably due to $I_M$.

rather than exclusively by $Ca^{2+}$ entering during the command. Fig. 15 also shows that this conclusion is independent of any $K^+$ accumulation that may have occurred during the voltage-clamp commands. If $K^+$ accumulation were sufficient to increase extracellular $K^+$ to 10 mM (an arbitrary but not unreasonable figure), $E_K$ would have been shifted to −67 mV. Such a shift would have little effect on the relation between peak conductance and command potentials. It would, however, mask the contribution of $I_K$ to the net outward current ($I_N$) since the conductance of the $I_K$ tail current would be underestimated.

### $I_M$

Between −120 and −20 mV, both kinetic and steady-state properties of $I_M$ are described by the Boltzman distribution predicted for a model where $I_M$ is regulated

by a voltage-sensing particle with a valency of 2·5 and a half-maximal activation voltage of −35 mV (see Adams *et al.* 1982*a*). Such a model predicts that the rate of opening and closing of $I_M$ have equal and opposite voltage sensitivities. Adams *et al.* (1982*a*) were unable, however, to test this aspect of the model because activation of much larger outward currents, $I_C$ and $I_K$ prevented the measurement of $I_M$ kinetics

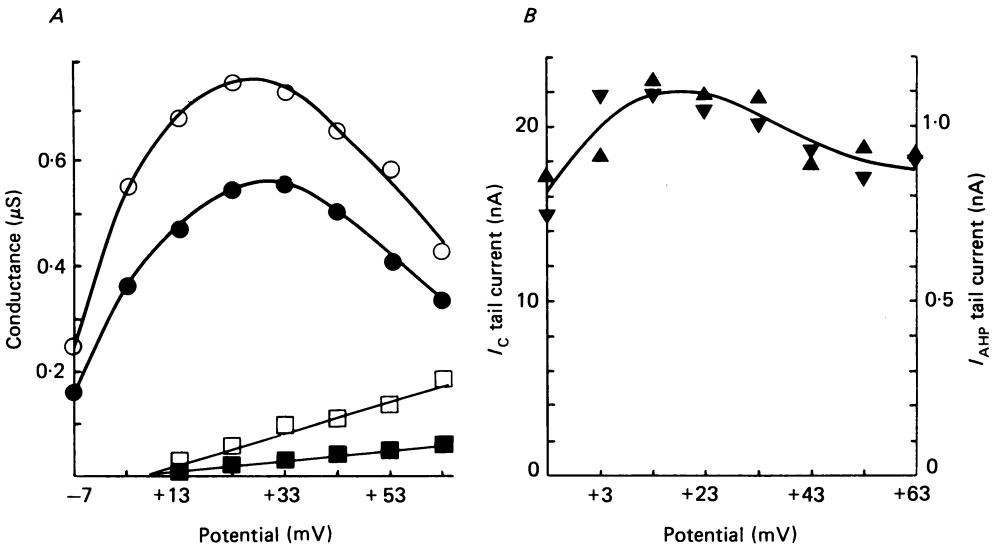


Fig. 15. Influence of command potential on the conductance at the end of a 2 ms command and on the magnitude of $I_C$, $I_K$ and $I_{AHP}$ components of the corresponding tail current. Same cell and conditions as in Fig. 14. *A*, conductance at the end of a 2 ms command plotted *vs.* command potential. For comparison amplitudes of the $I_K$ component of the corresponding tail current are converted to a conductance and plotted as well. Conductance calculated from $I_N$ (circles) and $I_K$ (squares) assuming $E_K = -106$ mV (closed symbols) or −67 mV (open symbols). *B*, amplitudes of $I_C$ (▼) and $I_{AHP}$ (▲) components of tail currents plotted *vs.* the corresponding command potential. *A*, $\tau_C = 2{\cdot}2$ ms, $\tau_K = 35$ ms, $\tau_{AHP} = 155$ ms.

at potentials positive to −20 mV. If true, however, an appreciable fraction of $I_M$ could be activated by brief voltage-clamp commands provided the commands were to sufficiently positive potentials. For example 25 % of $I_M$ channels would be activated by a 2 ms command to +40 mV and 80 % should be activated by a 2 ms command to +75 mV. In order to test this prediction, we attempted to measure the rate of activation of $I_M$ at positive potentials.

Experiments were carried out in 25 mM-$K^+$ to reduce distortions due to $K^+$ accumulation. $Ca^{2+}$ was removed and $Cd^{2+}$ (0·2 mM) was added to minimize distortion introduced by $I_C$ and $I_{AHP}$. Octanol (1 mM) was added to inhibit $I_K$ (we find that octanol causes a rapid and reversible blockade of $I_K$ without reducing $I_M$; moreover, the action of octanol is not voltage sensitive). Otherwise the medium was the same as that used by Adams *et al.* (1982*a*) (solution E).

Both steady-state and kinetic properties of $I_M$ were identical in solutions E and F and almost identical to those reported by Adams *et al.* (1982*a*). The only major

difference was an increased maximal conductance in solution F which is predicted by the constant-field theory since $K^+$ levels are higher (P. Pennefather, submitted for publication).

Fig. 16 shows a typical result. The rate of activation of $I_M$ was determined from the growth of an $I_M$ component of tail currents following commands of increasing

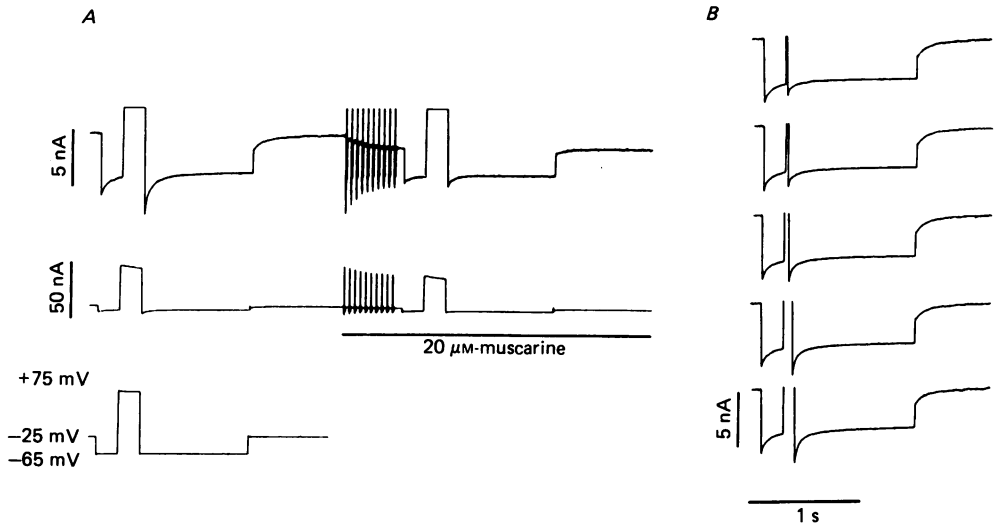


Fig. 16. Activation of $I_M$ by voltage-clamp commands to +75 mV. *A*, effect of muscarine on currents activated by a 200 ms command to +75 mV in solution F. Upper and middle trace are high- and low-gain records of currents. In the middle of these traces the chart speed was decreased 100-fold. The bottom traces shows the sequence of voltage-clamp commands. The command to +75 mV is given during a command to −65 mV from holding potential of −25 mV. Muscarine (20 μM) reduces the slow relaxations at the beginning and end of the command to −65 mV and at the end of the command to +75 mV. Thus the major slow component of the tail currents in solution F is $I_M$. *B*, effect of command duration on $I_M$ activated by commands to +75 mV. From top to bottom, command durations were: 10, 20, 40, 80 and 100 ms. Very little $I_M$ is activated by the 10 ms command, activation is still not maximal with the 100 ms command.

duration or from the time course of the difference current between outward currents recorded in the presence and absence of sufficient muscarine to maximally block $I_M$. Although details of this analysis will be presented elsewhere (P. Pennefather, submitted for publication), the conclusion was that the rate of activation of $I_M$ was much less voltage sensitive than the rate of closing. This is evident in Fig. 16 where a 10 ms command to +75 mV produces much less of a slow $I_M$ tail current than is produced by a 200 ms command that maximally activates $I_M$. Only 20% of total $I_M$ is activated by a 10 ms command to +75 mV. Extrapolation of the data predicts that only 5% of $I_M$ would be activated by a 2 ms command to +75 mV. This suggests that little $I_M$ will be activated during a single action potential.

## DISCUSSION

### *Separation of currents activated by brief depolarizations*

The experiments described here were designed to separate the various components of outward membrane current evoked by short depolarizing commands. The purpose of this was to determine the conductances which may be active or activated during an action potential. Of the currents detected, $I_M$ and $I_{AHP}$, are easily separated from $I_C$ and $I_K$ because of their small size and much slower rate of decay. $I_{AHP}$ is separable from $I_M$ on the basis of voltage-independent kinetics, $Ca^{2+}$ dependence and different pharmacological sensitivity. Similarly, $I_C$ can be separated from $I_K$ on the basis of $Ca^{2+}$ dependence. $Cd^{2+}$ produces a selective effect on the $Ca^{2+}$-sensitive component of outward current. However, it was often difficult to obtain a recovery following exposure to $Cd^{2+}$. Removal of $Ca^{2+}$ from the medium reversibly abolishes $I_C$ but this method is not completely satisfactory since there are subsequent alterations in the kinetics of the $I_K$.

The effect of zero $Ca^{2+}$, 4 mM-$Mg^{2+}$ Ringer solution to increase the peak amplitude of the $I_K$ tail would be consistent with a scheme whereby $Ca^{2+}$ normally screened surface electronegative charges in the vicinity of $I_K$ channels and reduced the extracellular surface potential. Removal of $Ca^{2+}$ then would make the extracellular surface potential more negative, reduce the transmembrane potential sensed by $I_K$ channel and in this way act like a depolarization (Frankenhaeuser & Hodgkin, 1957; McLaughlin, Szabo & Eisenman, 1971). The observation that $Mg^{2+}$ does not replace $Ca^{2+}$ in this regard would imply that discrete binding sites, with a higher affinity for $Ca^{2+}$ then $Mg^{2+}$, are involved (see Hille, Woodhull & Shapiro, 1975). Such a scheme would, however, predict that $I_K$ tail currents be slower after $Ca^{2+}$ was removed. In fact $I_K$ tail current decayed faster after removal of $Ca^{2+}$. This latter observation implies that a simple removal of charge screening is not a sufficient explanation for these effects. Replacement of $Ca^{2+}$ with $Mg^{2+}$ has no effect on the kinetics of another voltage-dependent current, $I_M$ (Adams *et al.* 1982*a*). Thus, $Ca^{2+}$ or $Mg^{2+}$ must be having a specific effect on $I_K$ (see also Armstrong & Matteson, 1986). As a result of this effect, it is of note that if only the difference in outward currents were considered, one might conclude that the $Ca^{2+}$-dependent outward current was transient.

Because of the difficulties involved in pharmacologically separating $I_C$ and $I_K$ we relied heavily on kinetic differences to distinguish between the two currents. We have shown that the major fast component of the $K^+$ tail current reflects $I_C$ while the major slow component is generated by $I_K$. For example $Cd^{2+}$ reduces the fast component without affecting the slow component and the amplitude of the slow component parallels the delayed onset of outward current seen in the presence of $Cd^{2+}$.

Using these methods we have determined that the action potential repolarization in bull-frog sympathetic neurones is due primarily to the activation of $I_C$ and under normal conditions is not significantly dependent upon activation of the delayed rectifier. The latter conclusion can be drawn for two reasons: $I_K$ is activated with too great a delay when one considers the voltage range covered by an action potential. This is despite the fact that many of the experiments described here were carried out in conditions favourable for the activation of $I_K$; i.e. elevated extracellular $K^+$. Thus even allowing for *in situ* $K^+$ accumulation which could easily occur after a single action potential, $I_K$ contribution to repolarizing of the action potential is likely to be small or zero. The $Na^+$ current inactivates rapidly in bull-frog ganglion cells (Jones, 1985) and should be mostly inactivated before the end of a normal action potential. Blockade of $I_{Ca}$ approximately doubles the action potential duration (see

Adams *et al.* 1982*c*; MacDermott & Weight, 1982). This suggests that a depolarization twice as long as a normal action potential would be required to activate sufficient $I_K$ to recharge the membrane potential.

MacDermott & Weight (1982) have described a transient, $Ca^{2+}$-dependent outward current that is mostly inactivated at −40 mV, but can be activated by depolarizing commands from hyperpolarized potentials. On the few occasions that we looked for this current by stepping to 0 mV from −80 mV, it was not observed. Regardless, the reported magnitude of the current (see also Brown, Constanti & Adams, 1982) is relatively small compared to $I_C$ and its role in spike repolarization remains to be determined. It is worth mentioning in passing that another transient outward current (A-current) is unlikely to be involved in spike repolarization bull-frog sympathetic neurones as reported for rat sympathetic neurones (Belluzi, Sacchi & Wanke, 1985*a*). In the bull-frog cells, A-current is mostly inactivated at typical resting potentials.

### $I_C$

The main current activated by action-potential-like depolarizations ($I_C$) is clearly a non-inactivating conductance over the first 50–60 ms. Experimental conditions were chosen to eliminate artifactual means of producing transient currents. Reduction of $K^+$ accumulation prevents large decreases in driving force during the command which causes declines in membrane current independent of conductance changes. Secondly, removal of $Na^+$ prevented axonal spikes which may generate remote outward currents. A further factor is poor voltage control (as opposed to poor space clamp) such that at the beginning of the pulse there is a slight overshoot of the potential from the actual command voltage. This is of concern because of the strong voltage dependence of $Ca^{2+}$ currents which is about e-fold per 8 mV in these cells (Adams *et al.* 1982*b*). Hence only a small transient voltage overshoot would be needed to generate a larger $Ca^{2+}$ current at the start of a command than at later times and therefore a larger outward current at the start of the command than at steady state. A similar transient activation of $I_{Ca}$ would occur if series resistance were appreciable since the large increases in conductance reported here take a few milliseconds to reach steady-state values. The fact that transient outward currents were not observed, suggests that the membrane potential was well clamped and not contaminated by remote spikes or series-resistance problems.

$I_C$ in bull-frog ganglia appears to be comparable to a $Ca^{2+}$-activated $K^+$ current in cockroach central neurones which has a similarly rapid activation and voltage sensitivity (Thomas, 1984); and to $I_C$ in rat sympathetic neurones (Galvan & Sedlmeir, 1984) and hippocampal neurones (Brown & Griffith, 1983) based on the $Ca^{2+}$ dependence and TEA sensitivity. Large-conductance ($\simeq$ 200 pS) $Ca^{2+}$-activated $K^+$ channels have been observed in chromaffin cells (Marty, 1981), clonal pituitary cells (Wong, Lecar & Adler, 1982), rat muscle cells (Pallotta *et al.* 1981), bull-frog and rat sympathetic neurones (Adams *et al.* 1982*b*; Smart, 1985) and rat hippocampal neurones (Brett & Lancaster, 1985). The voltage dependence and sensitivity to external TEA make it likely that the macroscopic $I_C$ current is the manifestation of the opening of these large conductance channels (see Adams *et al.* (1982*c*) for a direct comparison).

Detailed kinetic analysis of such channels at the single-channel level has led to the

recognition of certain characteristic properties (see Moczydlowski & Latorre, 1983; Magleby & Pallotta, 1983). Both the open time and closed time are $Ca^{2+}$ and voltage sensitive and the probability of being open exhibits a Hill coefficient of around 2 in its relation with $[Ca^{2+}]_i$. The data suggest that each channel is associated with at least two $Ca^{2+}$ binding sites; binding of the first calcium ion allows the channel to open, binding of the second calcium ion holds the channel open. Since the voltage sensitivity of channel open and closed time disappears at high $Ca^{2+}$, it seems likely that binding, rather than channel isomerization, is the voltage-dependent step.

The voltage sensitivity reported here (e-fold per 39 mV) is less than observed in B cells for $I_C$ relaxation activated by ionophoretic injection of $Ca^{2+}$ (e-fold per 22 mV). In the latter case, $Ca^{2+}$ was extensively buffered before reaching the cell membrane and did not activate much $I_C$ (see Adams *et al.* 1982*c*). The observation that voltage sensitivity of $I_C$ relaxations was less than that observed at low $Ca^{2+}$ levels implies that following brief commands, $[Ca^{2+}]_i$ near the cytosolic surface of the cell membrane can reach levels sufficient to begin to saturate the $Ca^{2+}$ binding site that regulates channel open time. The affinity of $Ca^{2+}$ for the site that regulates the frequency of channel opening must, however, be much less since the channels close at $-40$ mV. Indeed, the data of Moczydlowski & Latorre (1983) on the $Ca^{2+}$ sensitivity of analogous channels derived from rat muscle are best fitted if the two sites have dissociation constants for $Ca^{2+}$ that differ by a factor of 10 (see also Magleby & Pallotta, 1983).

With excised patches of rat muscle membrane (Barrett, Magleby & Pallotta, 1982) the open time of $I_C$-like channels has a greater voltage dependence than described here when 1 $\mu$M-$Ca^{2+}$ is present (see also Wong *et al.* 1982) but has less voltage sensitivity in 100 $\mu$M-$Ca^{2+}$. This suggests that following brief commands $I_C$ channels are exposed to intracellular $Ca^{2+}$ concentration of the order of $10^{-5}$ M. However, for the observed $Ca^{2+}$ current of a few nanoamperes (Adams *et al.* 1982*b*; P. R. Adams, unpublished observation) to generate such a concentration in B cells (radius 25 $\mu$m), $Ca^{2+}$ would have to be restricted to a layer extending approximately 1 $\mu$m from the inner membrane surface. The calculations of Zucker & Stockbridge (1983) suggest that because of buffered diffusion, $Ca^{2+}$ will not diffuse much further than 1 $\mu$m in the time taken for $I_C$ tail currents to be generated by 2–3 ms commands. This assumes that the buffering power of B cell cytoplasm is similar to that of squid axoplasm.

A word of caution is in order in comparing the $Ca^{2+}$ sensitivity of $I_C$-like channels in different preparations. Besides possible differences in the channels themselves, $I_C$-like channels sense a portion of the membrane surface potential (Moczydlowski, Alvarez, Vergara & Latorre, 1985), which may vary from cell type to cell type. Nevertheless, it seems clear that activation of $I_C$ in bull-frog ganglion cells is representative of the process in other types of neurones.

Because $I_C$ channels are both voltage and $Ca^{2+}$ sensitive it is possible that with a sufficiently positive command $I_C$ might be activated by voltage alone. Indeed even in the presence of $Cd^{2+}$ a small $I_C$-like component is observed in the tail current provided voltage-clamp commands are sufficiently positive. However, this result could also be obtained if the $Cd^{2+}$ blockade of $Ca^{2+}$ channels were voltage dependent (see Brown, Tsuda & Wilson 1983; Lansman, Hess & Tsien, 1986).

We have presented circumstantial evidence for a contribution of $Ca^{2+}$ tail current

to the $Ca^{2+}$ influx evoked by brief depolarization commands. Such an interpretation can account for the observation that both $I_C$ and $I_{AHP}$ components of the tail current reach a limiting value after commands to potential above those in the negative conductance region of the current–voltage relation. $Ca^{2+}$ entry during these commands is presumably negligible. The transient increase in $Ca^{2+}$ current during repolarization of the spike and subsequent activation of $I_C$ will oppose the tendency of $I_C$ to close too quickly and acts in a sense like a governor. The relative amounts of $Ca^{2+}$ entering during the command or during the tail current is a function of both the driving force for the $Ca^{2+}$ current at the two potentials and the duration of the command. With a 13 ms command to +30 mV (Fig. 8) most of the $Ca^{2+}$ entry will be during the command. While with a 13 ms command to +100 mV, most will enter during the tail current.

Since $I_{Ca}$ inactivates only very slowly (Adams *et al.* 1982*b*), the fact that $I_C$ reaches a steady-state value (Figs. 8 and 11) must reflect the action of intracellular $Ca^{2+}$ buffers to prevent $Ca^{2+}$ levels from rising excessively (see Adams *et al.* 1982*c*; Byerly & Moody, 1984). Within a few milliseconds of activating $Ca^{2+}$ channels, a new steady state is established between $Ca^{2+}$ influx and uptake onto buffer sites.

### $I_{AHP}$

Unlike $I_C$, $I_{AHP}$ is voltage insensitive, much less sensitive to blockade by TEA and is blocked by apamin (see Pennefather *et al.* 1985*b*). Recently, Blatz & Magleby (1986) have identified in rat myotubes a small (12 pS), $Ca^{2+}$-dependent $K^+$ channel which is additionally apamin sensitive. This channel was found to be voltage insensitive and at −40 mV about 10 times more $Ca^{2+}$ sensitive than the large-conductance $Ca^{2+}$-activated $K^+$ channel ($I_C$-like).

A greater sensitivity to $Ca^{2+}$ of $I_{AHP}$ channels would explain how the time course of $I_{AHP}$ decay could be so much different from that of $I_C$. Whereas $I_C$ decay would reflect the voltage-dependent dissociation of $Ca^{2+}$ from a binding site, $I_{AHP}$ decay would reflect the rate of removal or buffering of $Ca^{2+}$ injected during the depolarization. This conclusion is supported by the slow decay of $I_C$ in B cells evoked by intracellular ionophoresis of $Ca^{2+}$ (Adams *et al.* 1982*c*) and direct measurement of $[Ca^{2+}]_i$ using arzenazo III (Smith, MacDermott & Weight, 1983). The slow removal of $Ca_i^{2+}$ has been proposed to account for the time course of slow a.h.p.s in molluscan neurones as well (Eckert & Tillotson, 1978; Gorman & Thomas, 1980; Barish & Thompson, 1983; Deitmer & Eckert, 1985). Slow removal of $Ca_i^{2+}$ implies that the mean intracellular $Ca^{2+}$ levels are essentially constant during the decay of $I_C$ tail currents.

The magnitude of the slow a.h.p. was quite variable from cell to cell. It is our impression that cells with prominent a.h.p.s are ones that have escaped much damage during impalement rather than representing an anatomically distinct subgroup. Small a.h.p.s were generally associated with a low input resistance which would tend to shunt the current responsible for the a.h.p. (Adams, Pennefather & Lancaster, 1985). Also, the underlying a.h.p. current tended to be small in cells with a low input resistance; the a.h.p. current appeared to be quite labile. It is of note that small C cells of the bull-frog ganglion (see Dodd & Horn, 1983) do not exhibit as prominent an a.h.p. as B cells even when input resistance is high (S. W. Jones, personal

communication). The lability of $I_{AHP}$ might reflect rundown of the $Ca^{2+}$ current, a commonly observed phenomenon; however, $I_{AHP}$ can be absent in cells that show a robust $I_C$. It is possible that any elevation of intracellular $Ca^{2+}$ levels, such as $Ca^{2+}$ loading purely through impalement leak, may fully activate $I_{AHP}$ at rest. However, apamin has little effect on holding current even when cells have small a.h.p.s (unpublished observations).

*$I_M$*

It is clear from Fig. 16 that brief commands activate little $I_M$ even when the commands are very large. A detailed description of this phenomenon will be presented elsewhere (P. Pennefather, submitted for publication). At this point, it is sufficient to note that little $I_M$ will be activated by individual action potentials.

*$K^+$ accumulation*

Fluctuations in extracellular $K^+$ proved to be a major problem in the analysis of our data. Two approaches were taken in order to deal with this problem. The first involved raising the level of extracellular $K^+$ in an attempt to dampen the influence of $K^+$ accumulation on the time course of $K^+$ currents. However, this approach changed the gating properties of $I_K$. Until the effects of ions on $I_K$ are fully described, it will be difficult to deduce the kinetics of $I_K$ under normal conditions from experiments carried out in abnormal ionic conditions. The second approach, was to monitor $E_K$ during the development of a current in order to calculate the change of chord conductance with time. This proved to be rather tedious although not impossible. The approach is still not very satisfactory since extracellular $K^+$ is changing in an uncontrolled way. A third approach that we hope to pursue in the future is to repeat our experiments using isolated cells obtained by the enzymatic dispersal of ganglia (see Jones, 1985). Ultimately, however, it will be necessary to verify that data obtained in isolated cells are applicable to what goes on in the intact ganglion.

We attempted to model the $K^+$ accumulation process. Although this model is rather simplistic, it provides some insight into the phenomenon. It predicts that if the restricted space is evenly distributed over the surface of a B cell, it would have a width of 30–50 nm. This would appear to correspond to the space between the neurone surface and the layer of satellite cells that encapsulate the neurone (Taxi, 1976; Wantanabe, 1983). The model also predicts that the steady-state level of extracellular $K^+$ will be a linear function of outward current. This is what has been observed by Belluzi, Sacchi & Wanke (1985*b*) in the rat sympathetic ganglion, which is also encapsulated with satellite cells (Dail & Barton, 1983). With brief commands, $K^+$ accumulates with a rate constant between 50 and 100 $s^{-1}$, so that between 10 and 20% of the steady-state levels of extracellular $K^+$ could accumulate within 2 ms. Since brief action-potential-like depolarizations can evoke about 100 nA of outward current which at equilibrium will cause accumulation of at least 30 mM-$K^+$ (see also Belluzzi *et al.* 1985*b*), it is clear that extracellular $K^+$ may double or even triple during a single action potential.

It is of interest that Stimers, Bezanilla, Taylor & Webb (1985), who have also studied the relation between $E_K$ and outward current, concluded that the

Frankenhaeuser–Hodgkin space of squid axon had dimensions and properties similar to those described here. Significant $K^+$ accumulation may be a general feature of neurones that are surrounded by glia. An outward current of 100 nA at +20 mV in the bull-frog ganglion cells corresponds to about 1 channel/$\mu m^2$; this density seems typical for $I_C$ in many cell types. The restricted space created by a glial sheath will be proportional to cell surface area. As a result, $K^+$ accumulation will reflect current density rather than absolute current.

The authors would like to thank Paul R. Adams for his advice and encouragement throughout the course of this work, and for the use of laboratory facilities; also, Steven W. Jones for comments on the manuscript. This work was funded by grants NS 18597 to P. R. Adams and MNA-9604 to P. Pennefather. P. Pennefather was supported by a Killam Postdoctoral Fellowship and a Career Scientist award from the Ontario Ministry of Health. B. Lancaster received a travel grant from the Wellcome Trust.

## REFERENCES

ADAMS, P. R., BROWN, D. A. & CONSTANTI, A. (1982*a*). M-currents and other potassium currents in bullfrog sympathetic neurones. *Journal of Physiology* **330**, 537–572.

ADAMS, P. R., BROWN, D. A. & CONSTANTI, A. (1982*b*). Voltage clamp analysis of membrane currents underlying repetitive firing of bullfrog sympathetic neurons. In *Physiology and Pharmacology of Epileptogenic Phenomena*, ed. KLEE, M. R., LUX, H. D. & SPECKMANN, E. J. New York: Raven Press.

ADAMS, P. R., CONSTANTI, A., BROWN, D. A. & CLARK, R. B. (1982*c*). Intracellular $Ca^{2+}$ activates a fast voltage-sensitive $K^+$ current in vertebrate sympathetic neurones. *Nature* **296**, 746–749.

ADAMS, P. R., JONES, S. W., PENNEFATHER, P., BROWN, D. A., KOCH, C. & LANCASTER, B. (1986). Slow synaptic transmission in frog sympathetic ganglia. *Journal of Experimental Biology* **124**, 259–285.

ADAMS, P. R., PENNEFATHER, P. & LANCASTER, B. (1985). Spike after hyperpolarization (AHPs) in bullfrog sympathetic ganglion 'B' cells. *Biophysical Journal* **47**, 387*a*.

AKAIKE, N., LEE, K. S. & BROWN, A. M. (1978). The calcium current of *Helix* neuron. *Journal of General Physiology* **71**, 509–531.

ARMSTRONG, C. M. & MATTESON, D. R. (1986). The role of calcium ions in the closing of K channels. *Journal of General Physiology* **87**, 817–832.

BARISH, M. E. & THOMPSON, S. H. (1983). Calcium buffering and slow recovery kinetics of calcium dependent outward current in molluscan neurones. *Journal of Physiology* **337**, 201–219.

BARRETT, J. N., MAGLEBY, K. L. & PALLOTTA, B. S. (1982). Properties of calcium-activated potassium channels in cultured rat muscle. *Journal of Physiology* **331**, 211–230.

BELLUZZI, O., SACCHI, O. & WANKE, E. (1985*a*). A fast transient outward current in the rat sympathetic neurone studied under voltage-clamp conditions. *Journal of Physiology* **358**, 91–108.

BELLUZZI, O., SAACHI, O. & WANKE, E. (1985*b*). Identification of delayed potassium and calcium currents in the rat sympathetic neurone under voltage clamp. *Journal of Physiology* **358**, 109–129.

BLATZ, A. L. & MAGLEBY, K. L. (1986). Single apamin-blocked Ca-activated $K^+$ channels of small conductance in cultured rat skeletal muscle. *Nature* **323**, 718–720.

BRETT, R. S. & LANCASTER, B. (1985). Activation of potassium channels by rapid application of calcium to inside-out patches of cultured hippocampal neurons. *Society for Neuroscience Abstracts* **11**, 954.

BROWN, A. M., TSUDA, Y & WILSON, D. L. (1983). A description of activation and conduction in calcium channels based on tail and turn-on current measurements in the snail. *Journal of Physiology* **344**, 549–583.

BROWN, D. A., CONSTANTI, A. & ADAMS, P. R. (1982). Calcium-dependence of a component of transient outward current in bullfrog ganglion cells. *Society for Neuroscience Abstracts* **8**, 252.

BROWN, D. A. & GRIFFITH, W. H. (1983). Calcium-activated outward current in voltage-clamped hippocampal neurones of the guinea-pig. *Journal of Physiology* **337**, 287–301.

BYERLY, L. & MOODY, W. J. (1984). Intracellular calcium ions and calcium currents in perfused neurones of the snail, *Lymnaea stagnalis*. *Journal of Physiology* **352**, 637–652.

DAIL, W. G. & BARTON, S. (1983). Structure and organization of the mammalian sympathetic ganglia. In *Autonomic Ganglia*, ed. ELFVIN, L. G., pp. 3–26. Toronto: John Wiley and Sons.

DEITMER, J. W. & ECKERT, R. (1985). Two components of Ca-dependent potassium current in identified neurones of *Aplysia californica*. *Pflügers Archiv* **403**, 353–359.

DODD, J. & HORN, J. P. (1983). A reclassification of B and C neurones in the ninth and tenth paravertebral sympathetic ganglia of the bullfrog. *Journal of Physiology* **334**, 255–269.

DUBOIS, J. M. (1981). Simultaneous changes in the equilibrium potential and potassium conductance in voltage clamped Ranvier node in the frog. *Journal of Physiology* **318**, 279–295.

ECKERT, R. & TILLOTSON, D. (1978). Potassium activation associated with intraneuronal free calcium. *Science* **200**, 437–439.

FENWICK, E. M., MARTY, A. & NEHER, E. (1982). Sodium and calcium channels in bovine chromaffin cells. *Journal of Physiology* **331**, 599–635.

FRANKENHAEUSER, B. (1962). Delayed currents in myelinated nerve fibres of *Xenopus laevis* investigated with voltage clamp technique. *Journal of Physiology* **160**, 40–45.

FRANKENHAEUSER, B. & HODGKIN, A. L. (1957). The action of calcium on the electrical properties of squid axons. *Journal of Physiology* **137**, 218–244.

GALVAN, M. & SEDLMEIR, C. (1984). Outward currents in voltage clamped rat sympathetic neurones. *Journal of Physiology* **356**, 115–133.

GORMAN, A. L. F. & THOMAS, M. V. (1980). Potassium conductance and internal calcium accumulation in a molluscan neurone. *Journal of Physiology* **308**, 287–313.

HAGIWARA, S. & OHMORI, H. (1982). Studies of calcium channels in rat clonal pituitary cells with patch electrode voltage clamp. *Journal of Physiology* **331**, 231–252.

HILLE, B., WOODHULL, A. M. & SHAPIRO, B. I. (1975). Negative surface change near sodium channels of nerve: divalent ions, monovalent ions, and pH. *Philosophical Transactions of the Royal Society B* **270**, 301–308.

HODGKIN, A. L. & HUXLEY, A. F. (1952). Currents carried by sodium and potassium ions through the membrane of the giant axon of *Loligo*. *Journal of Physiology* **116**, 449–472.

HODGKIN, A. L. & KATZ, B. (1949). The effect of sodium ions on the electrical activity of the giant axon of the squid. *Journal of Physiology* **108**, 37–77.

JONES, S. W. (1985). The sodium current of dissociated bullfrog sympathetic neurons. *Society for Neuroscience Abstracts* **11**, 314.

LANCASTER, B., PENNEFATHER, P. & ADAMS, P. R. (1985). Voltage clamp analysis of rapidly activating potassium currents in bullfrog sympathetic ganglion cells. *Society for Neuroscience Abstracts* **11**, 787.

LANSMAN, J. B., HESS, P. & TSIEN, R. W. (1986). Blockade of currents through single calcium channels by $Cd^{2+}$, $Mg^{2+}$ and $Ca^{2+}$ voltage–concentration dependence of calcium entry into the pore. *Journal of General Physiology* **88**, 321–347.

LEE, K. S. & TSIEN, R. W. (1982). Reversal of current through calcium channels in dialysed single heart cells. *Nature* **297**, 498–501.

MACDERMOTT, A. B. & WEIGHT, F. F. (1982). Action potential repolarization may involve a transient, $Ca^{2+}$-sensitive outward current in a vertebrate neurone. *Nature* **300**, 185–188.

MCLAUGHLIN, S. G. A., SZABO, G. & EISENMAN, G. (1971). Divalent ions and the surface potential of charged phospholipid membranes. *Journal of General Physiology* **58**, 667–687.

MAGLEBY, K. L. & PALLOTTA, B. S. (1983). Calcium dependence of open and shut interval distribution from calcium-activated potassium channels in cultured rat muscle. *Journal of Physiology* **344**, 585–604.

MARTY, A. (1981). Ca-dependent K channels with large unitary conductance in chromaffin cell membranes. *Nature* **291**, 497–500.

MARTY, A. & NEHER, E. (1985). Potassium channels in cultured bovine adrenal chromaffin cells. *Journal of Physiology* **367**, 117–141.

MEECH, R. W. & STANDEN, N. B. (1975). Potassium activation in *Helix aspersa* neurones under voltage clamp: a component mediated by calcium influx. *Journal of Physiology* **249**, 211–239.

MOCZYDLOWSKI, E., ALVAREZ, O., VERGARA, C. & LATORRE, R. (1985). Effect of phospholipid surface charge on the conductance and gating of a $Ca^{2+}$-activated $K^+$ channel in planar lipid bilayers. *Journal of Membrane Biology* **83**, 273–282.

MOCZYDLOWSKI, E. & LATORRE, R. (1983). Gating kinetics of $Ca^{2+}$ activated $K^+$ channels from rat

muscle incorporated into planar lipid bilayers. Evidence for two voltage dependent $Ca^{2+}$ binding reactions. *Journal of General Physiology* **82**, 511–542.

PALLOTTA, B. S., MAGLEBY, K. L. & BARRETT, J. N. (1981). Single channel recordings of $Ca^{2+}$-activated $K^+$ currents in rat muscle cell culture. *Nature* **293**, 471–474.

PENNEFATHER, P. (1986). The rate of activation of M current at positive potentials in bullfrog sympathetic ganglion cells. *Biophysical Journal* **49**, 166a.

PENNEFATHER, P., JONES, S. W. & ADAMS, P. R. (1985*a*). Modulation of repetitive firing in bullfrog sympathetic ganglion cells by two distinct K currents, $I_M$ and $I_{AHP}$. *Society for Neuroscience Abstracts* **11**, 148.

PENNEFATHER, P., LANCASTER, B., ADAMS, P. R. & NICOLL, R. A. (1985*b*). Two distinct Ca-dependent K currents in bullfrog sympathetic ganglion cells. *Proceedings of the National Academy of Sciences of the U.S.A.* **82**, 3040–3044.

REUTER, H. & SCHOLZ, H. (1977). A study of the ion selectivity and the kinetic properties of the calcium-dependent slow inward current in mammalian cardiac muscle. *Journal of Physiology* **264**, 17–47.

SMART, T. B. (1985). Single $Ca^{2+}$-activated $K^+$ channels recorded from cultured rat sympathetic neurones. *Journal of Physiology* **362**, 46*P*.

SMITH, S. J., MACDERMOTT, A. B. & WEIGHT, F. F. (1983). Detection of intracellular $Ca^{++}$ transients in sympathetic neurons using arsensazo III. *Nature* **304**, 350–352.

STIMERS, J. R., BENZANILLA, F., TAYLOR, R. E. & WEBB, C. (1985). Sodium gating currents without rising phases: evidence from potassium currents. *Biophysical Journal* **49**, 384a.

STORM, J. (1985). Calcium-dependent spike repolarization and three kinds of afterhyperpolarization (AHP) in hippocampal pyramidal cells. *Society for Neuroscience Abstracts* **11**, 1183.

TAXI, J. (1976). Morphology of the autonomic nervous system. In *Frog Neurobiology*, ed. LLINÁS, R. & PRECHT, W., pp. 93–150. Berlin: Springer-Verlag.

THOMAS, M. V. (1984). Voltage-clamp analysis of a calcium-mediated potassium conductance in cockroach (*Periplaneta americana*) central neurones. *Journal of Physiology* **350**, 159–178.

WANTANABE, H. (1983). The organization and fine structure of autonomic ganglia of amphibia. In *Autonomic Ganglia*, ed. ELVIN, L. G., pp. 183–202. Toronto: John Wiley & Sons.

WONG, B. S., LECAR, H. & ADLER, M. (1982). Single calcium dependent potassium channels in clonal anterior pituitary cells. *Biophysical Journal* **39**, 313–317.

ZUCKER, R. & STOCKBRIDGE, N. (1983). Presynaptic calcium diffusion and the time course of transmitter release and synaptic facilitation at the squid giant synapse. *Journal of Neuroscience* **3**, 1263–1269.